Proteomic and biomechanical properties of human menisci related to osteoarthritis

Kristina Gehrisch & Lykke Månsson

Lund, June 2021

LUND
UNIVERSITY

Master's Thesis in
Biomedical Engineering

Faculty of Engineering, LTH
Department of Biomedical Engineering

Supervisors: Neserin Ali, Hanna Isaksson, and Martin Englund

Title
Proteomic and biomechanical properties of human menisci related to osteoarthritis

Authors
Kristina Gehrisch & Lykke Månsson

Figures
Created by the authors if nothing else is indicated

Lunds Universitet
Institutionen för biomedicinsk teknik
Box 118
SE-221 00 Lund
Sverige

E-husets tryckeri
Lund 2021

Acknowledgements

We would first of all like to thank our supervisors, Neserin Ali, Hanna Isaksson and Martin Englund, for your guidance and support throughout this project. Thank you for always being reachable and providing us with the help we need, especially during a worldwide pandemic.

To the Clinical Epidemiology group, thank you for making us feel welcome and including us in your team from day one. A special appreciation to Jenny Lönsjö for her assistance and encouragement.

Finally, we would like to express our gratitude to Thomas Notermans and Anna Gustafsson for their technical support and patience with us when struggling with Matlab.

Abstract

Osteoarthritis is the most common form of arthritis and is expected to become even more prevalent worldwide with an increasingly older and more obese population. The degenerative joint disease, causing pain, swelling and stiffness in the joints, has a complex etiology and knowledge of the pathophysiological mechanisms is still limited. Recent studies have however reported that the meniscus plays an important role in the development of knee osteoarthritis.

The aim of this study was to gain new insight in knee osteoarthritis by implementing a multidisciplinary approach to study meniscal degradation. Thus, we specifically aimed to examine if there is an association between the protein content of a meniscus and its biomechanical properties.

Menisci from healthy and arthritic knees, both medial and lateral, were subjected to proteomic and biomechanical testing. 50 samples were prepared for mass spectrometry (Q Exactive HFX™) and for an unconfined compression test, 12 lateral menisci were selected. The protein content was obtained in the proteomic experiment whereas the elastic and aggregate modulus among other parameters could be calculated through the mechanical testing.

Results from the proteomic analysis of this study showed that medial menisci are more affected by osteoarthritis than lateral. Analysis of protein content presented an overall down regulation of glycoproteins and proteins involved in cell interaction in menisci from arthritic knees. The proteins CAH1, collagen type III and CILP2 were, among others, exhibited at higher levels in menisci from arthritic knees than healthy knees. These proteomic findings could not be connected to the biomechanical properties as these results showed no significant differences be-

tween healthy and osteoarthritic lateral menisci. Material modelling was performed using a Generalized Maxwell model and the biomechanical results showed a consistent increase in elastic modulus with increasing strain levels.

As the findings from this project showed that the medial menisci are more affected by osteoarthritis than the lateral, future biomechanical experiments and research should focus on medial menisci.

List of acronyms & abbreviations

ε - strain

ν - Poisson's ratio

σ - stress

BMI - body mass index

DDA - data dependent acquisition

DIA - data independent acquisition

E_s - Young's modulus

ECM - extra cellular matrix

GAG - glycosaminoglycan

H_A - aggregate modulus

LC - liquid chromatography

MS - mass spectrometry

OA - osteoarthritis

PCA - principal component analysis

SD - standard deviation

SLS - standard linear solid

LG - lateral menisci from healthy knees

LY - lateral menisci from arthritic knees

MG - medial menisci from healthy knees

MY - medial menisci from arthritic knees

Contents

Chapter 1

Introduction

Arthritis is one of the most frequent musculoskeletal diseases, affecting approximately one in four over the age of 45 in Sweden [1]. Arthritis occurs most frequently amongst elderly and overweight and risks becoming even more prevalent with a worldwide increasingly older and more obese population. Osteoarthritis (OA) is a degenerative form of arthritis where cartilage wears down, causing swelling, pain and stiffness in joints. The uncertainty of what causes OA is one of the biggest difficulties with prevention, diagnosis and treatment [2].

Another aspect that contributes to the complexity of OA is how differently it appears in patients. It is often the case that the radiographic evidence of the disease does not correspond to the patients' experienced pain which can allow OA to develop into an advanced stage, reducing the chances of improvement [3]. Apart from X-ray imaging, that can detect the breakdown of cartilage through a characteristic narrowing of the distance between the bones as well as the growth of bony spurs, MRI is another alternative when evaluating the condition of the cartilage [4]. There is currently no cure to OA but certain remedies can be implemented to help ease the pain, such as medications, exercise and lifestyle changes. In extreme cases where surgery is necessary, arthroplasty can be performed [5].

Research has found that the menisci play an important role concerning the etiology and pathogenesis of knee OA [6], opening up a possibility to study the meniscus' properties in order to gain deeper knowledge of the disease. To understand the course of OA, mapping the differences in both biological and mechanical properties between healthy and arthritic

menisci is of great value. The function and biological mechanism of tissues are highly dependent on the protein content and in order to analyse the proteome, mass spectrometry can be used. If dissimilarities are found between the proteins in healthy and OA-affected menisci, it could be a step in the right direction. These findings can then be related to the varying mechanical properties found in normal and degenerated menisci, explaining how OA develops and affects the tissue.

1.1 Aim

The aim of this thesis was to gain new insight in knee OA pathogenesis by implementing a multidisciplinary approach. Through a combined investigation into the proteomics of the meniscus as well as its biomechanical properties, the knowledge of prevention, diagnosis and treatment can hopefully be increased. This was performed by mapping the proteins and testing the compressive properties of menisci from donors with healthy knees and patients with varying degree of osteoarthritic knees. The relationship between the protein content and the biomechanical properties of the menisci were also investigated.

1.2 Design of the study

This project was a collaboration between the Clinical Epidemiology group (Dept. Clinical Sciences, Lund) and the Biomechanics group (Dept. Biomedical Engineering, Lund). 50 menisci, both lateral and medial, from 10 healthy and 15 OA-knees were available for this project, provided by the MENIX biobank (PI Prof Englund) at Skåne University Hospital. During the first part of the project, protein content of the menisci was determined using mass spectrometry. The second part consisted of unconfined biomechanical compression tests of the same menisci in those cases where enough tissue remained. Analysis was performed to investigate potential connections between protein content and biomechanical properties in menisci from healthy and arthritic knees.

1.3 Authors' contribution

The thesis consisted of two main elements, the protein content determination and the biomechanical experiment. Both authors were equally

involved in the two parts. However, the analyses were divided between the two authors to work as efficiently as possible. Kristina Gehrisch spent more time on creating the results of the biomechanical data in Matlab whereas Lykke Månsson spent more time on the protein content analysis and the Generalized Maxwell model. Close collaboration and discussions were always present between the two authors and they have equally contributed to the writing of the report.

Chapter 2

Background

2.1 Osteoarthritis (OA)

OA is a chronic degenerative joint disease primarily associated with the breakdown of cartilage. The main symptoms of OA are joint pain and stiffness, which often lead to musculoskeletal disability and an overall reduced quality of life. The disease is colloquially referred to as 'wear and tear' arthritis as it is often believed that the cartilage is worn down over time, however, the etiology of OA is multifactorial and can be derived through a combination of systemic and local features.

Systemic factors include age, gender and genetics. With an increasing age, the cartilage deteriorates causing a weakening of the joints' mechanical properties. Not only are women more prone to developing OA, studies also show that women often suffer more severe OA than men [4], perhaps explained with the difference in hormones and the musculoskeletal system. Research has suggested that 39%-65% of all OA cases can be derived through genetic factors [4].

Obesity, physical activity and joint injury are three fundamental local factors contributing to the development of OA. A high BMI has been shown to increase the risk of OA due to excess overloading and damage, especially to the knee joint. Physical activity, such as heavy lifting and repetitive occupational activity, has also been found to have a strong association with OA [7]. Injuries to the load bearing structures of the joints strongly increases the risk of developing OA at a later stage. This can especially be identified with traumatic meniscal tears causing

increased contact stress in the knee joint and breakdown of the cartilage. On the flip side, OA can also be the source of spontaneous meniscal degradation, resulting in tearing of the tissue. This creates a vicious cycle of biomechanical derangement and tissue changes [8].

2.1.1 Diagnosis

Apart from pain and stiffness, OA causes physiological changes within the joint such as joint space narrowing, formation of osteophytes (bone spurs) and stiffening of the bone which weakens its ability to absorb impact [4]. There is no clear method of identifying OA. Examination usually includes joint aspiration; mainly with the purpose of ruling out other medical conditions, X-ray imaging and MRI scans [4]. Through radiological imaging, some of the above mentioned features can be characterized, and, with the help of MRI, the cartilage in the joint can be visualized, contributing to a better understanding of the condition. MRI is especially useful for detecting meniscal tears [8].

2.1.2 Treatment

There is currently no cure for OA, there are however some treatments that can relieve pain and improve the function of the joint. Non-drug methods are normally the preferred initial treatment [9] and include patient education, supportive devices and physiotherapy. By incorporating lifestyle changes such as weight loss and appropriate exercise, patients may increase their quality of life. Drugs for pain relief and anti-inflammatory medicine can be recommended as a complement. In cases of advanced OA, joint replacement surgery, a type of arthroplasty, may be required [5].

Due to the lack of knowledge of OA in regards to etiology, further insight is necessary to prevent the increasing prevalence. Of all forms of OA, knee OA is the most diagnosed, accounting for over 80% of all cases [10]. Research has showed that the menisci play an important role concerning the pathogenesis of a certain phenotype of knee OA [6], enabling an opportunity to increase the knowledge of knee OA through investigation of how healthy and OA menisci differ.

2.2 Meniscus

2.2.1 Anatomy and composition

The menisci are located on the lateral and medial part in the knee, between the tibial plateau and the femoral condyle [5]. Their primary function is to transmit load across the tibiofemoral joint to decrease stresses on the articular cartilage. They are also important in stability, shock absorption, lubrication and nutrition to the knee joint. The menisci are crescent-shaped structures, however, the medial and the lateral meniscus are shaped slightly different, see figure 2.1. The meniscal horns, i.e. the outer parts, attach the menisci to the subcondral bone [11].

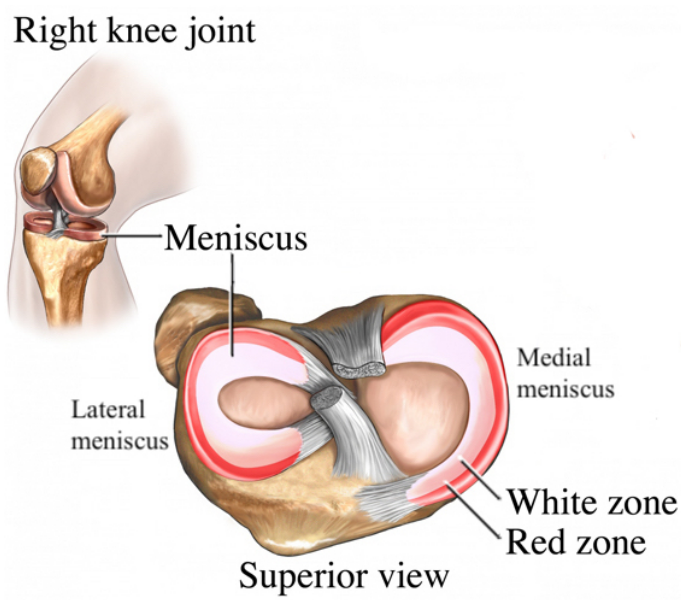

Figure 2.1: An anatomic overview of the medial and lateral meniscus [12].

Water makes up 72% of the meniscus' wet weight, the remaining 28% consists of collagen fibres (both type I and II), extracellular matrix and cells [5]. The body of the meniscus is typically divided into three segments and the biological composition differs depending on the location. Collagen type II is more prevalent in the two inner-thirds, also known as the white zone, whereas type I is more common in the peripheral third,

known as the red zone [5]. Depending on the depth of the meniscus' tissue, the orientation of the fibers differ. In the deep tissue, the fibers are circumferentially organized and gradually become more and more randomly oriented closer to the surface layer [5].

The compressive stiffness of the meniscus is predominantly provided by the presence of proteoglycans. These strongly hydrophilic proteins with glycosaminoglycan chains attached, absorb water and can therefore withstand strong compressive loads [13].

As previously mentioned, the lateral and the medial menisci are slightly different. The medial meniscus is not as circular as the lateral and its posterior horn is significantly broader than the anterior horn [14]. The lateral meniscus covers a larger area of the articular surface than the medial, 80% compared to 60%. The attachments of the lateral meniscus are not as developed as the medial, allowing the lateral meniscus to be more movable in all ranges of motion [15]. Since the medial meniscus is more firmly attached it is also more commonly injured [16].

2.2.2 Biomechanical properties

Due to the collagen network and the high water content, the meniscus tissue is viscoelastic [11]. A viscoelastic material incorporates a time element in its response to an external force. The loading and unloading curves for an elastic material are identical unlike the curves of a viscoelastic one. The time element in the response of a viscoelastic material causes the material to behave different during the loading and unloading, neither will the material return to its original shape immediately upon removing the external force. This will cause a loop when plotting the stress against the strain where the area between the loading and unloading represents the energy lost during the cycle, see figure 2.2 [17]. This energy is absorbed by the tissue, making it a good shock absorber [18] which is one of the meniscus' main purposes [11]. Another viscoelastic trait is that the material is strain rate dependent, the higher the loading rate, the higher the stiffness of the material [18]. Apart from strain rate dependency, the meniscus also exhibits an increasing stiffness as the strain increases.

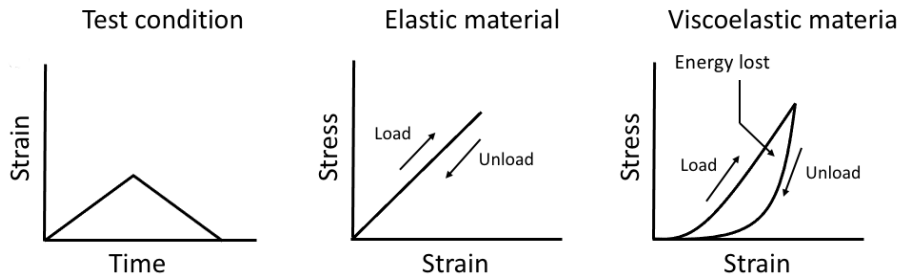

Figure 2.2: Elastic and viscoelastic behaviour when a material is loaded and unloaded.

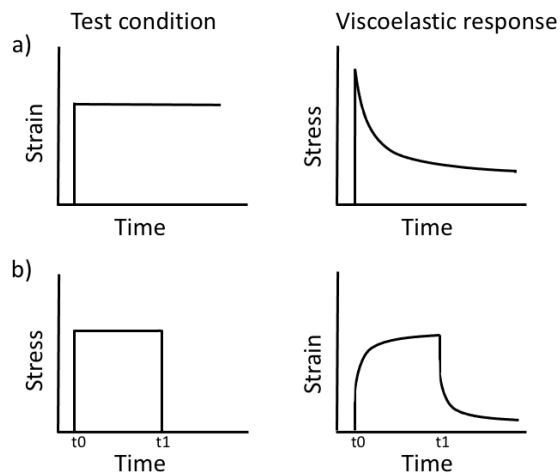

Figure 2.3: Visualization of the loading protocol and the viscoelastic response for a) stress relaxation and b) creep.

To investigate a viscoelastic tissue, time-dependent mechanical tests can be performed. The idea of these tests is to apply and hold either a constant force or displacement to see how the material responds over time. Holding a constant displacement is known as a stress relaxation test and holding a constant force is called a creep test, see a) and b) in figure 2.3. These mechanical tests are explained further in the section concerning biomechanical testing. Due to the strain dependent properties of a viscoelastic material, it is important to consider not only one, but several stress or strain values when performing biomechanical testing to form a complete representation of the material [17].

2.3 Mass spectrometry

To obtain the protein content from a sample, mass spectrometry (MS) can be performed. Sample preparation is a crucial step prior to MS-analysis in order to obtain reliable and high-quality results, this includes verifying factors such as concentration, volume, desalting and composition [19]. MS coupled with liquid chromatography (LC) allows separation of a sample's components through the compound's interaction with the mobile and stationary phase. The affinity to the mobile phase causes the compounds to separate over a gradient before entering the mass spectrometer [20], see figure 2.4.

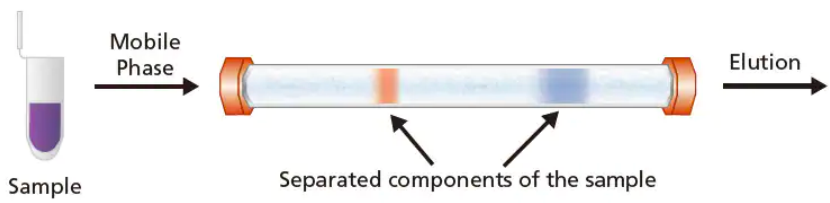

Figure 2.4: Liquid chromatography [21].

MS is an analytical technique that converts compounds and atoms into charged ions and measures their mass to charge (m/z) ratio [22]. A mass spectrometer consists of three main parts; an ionization source that converts the analyte molecules into gas-phase ions, a mass analyser that separates the ions based on their m/z ratio and a detector that records the number of ions at a certain m/z ratio [23], see figure 2.5.

The structure of these components vary depending on the purpose of the mass spectrometer, the required data and the sample properties. The molecules that are loaded into the mass spectrometer are vaporized and ionized in the ionization source. Because of their charge, the mass spectrometer can accelerate the ions throughout the rest of the system. When the ions reach the mass analyser, they encounter electric and/or magnetic fields making the paths of individual ions deflect depending on their m/z ratio. The ions that pass the deflection then hit the detector. Finally, the mass spectrometer is connected to a software that measures the ion oscillation frequencies and acquires a mass spectra [19].

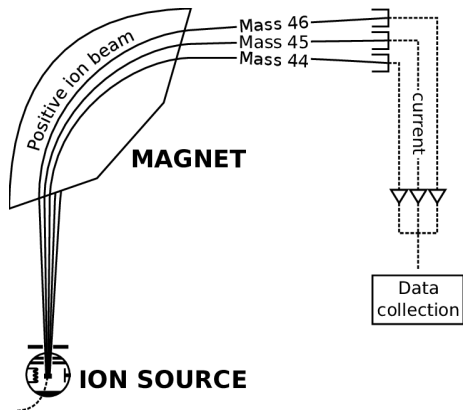

Figure 2.5: A schematic representation of a simple mass spectrometer [24].

Tandem mass spectrometry, also known as MS/MS, is a technique where a sample is either analysed by two or more mass spectrometers or by one mass spectrometer with several analysers [25]. The ions produced in the first MS are called precursor ions which in the second MS are broken down to product ions. MS/MS is a technique that is especially useful when sequencing peptides and proteins [23].

Data independent acquisition (DIA) and data dependent acquisition (DDA) are two methods of identifying the proteins/peptides in the samples. DDA is a procedure where all precursor ions are scanned during MS1. In MS2 a predefined number of precursor ions over a certain mass to charge threshold are selected for further fragmentation, see figure 2.6. This approach provides detailed peptide sequencing information about the selected precursor ions [26].

DIA is a developed proteomic strategy which provides better sensitivity and reproducibility compared to DDA. In DIA, all the precursor ions from MS1 are fragmented in isolated windows, see figure 2.6. Unlike DDA where only a selected range of precursor ions are fragmented, DIA allows for all detected precursor ions to be further analysed. However, DIA requires mass spectrometers capable of high resolution spectra acquisition at fast scan speeds [26].

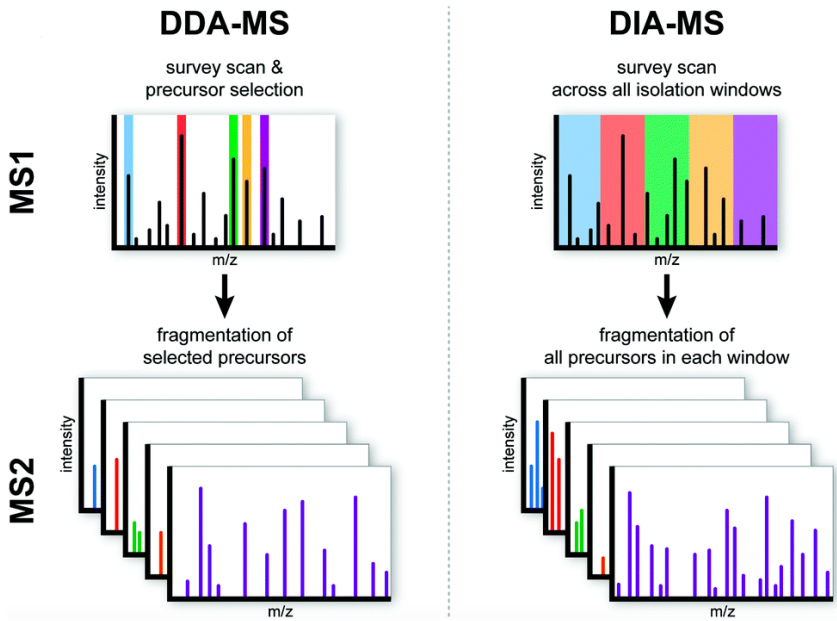

Figure 2.6: A schematic overview of DDA-MS and DIA-MS [26].

2.4 Biomechanical testing

Biomechanical testing can be performed to obtain biomechanical properties of tissues. Unconfined compression is a popular technique to use when performing mechanical compression testing on cylindrical-shaped samples. During the test, a sample is compressed between two flat plates, allowing the sample to expand in the radial direction. The test can be controlled by force or displacement where the latter is more common. Parameters obtained from the test are normally displacement, force and time. By dividing the force with the cross-sectional area of the sample, and the displacement by the length of the sample, stress, σ, and strain, ϵ, can be calculated, see equations (2.1) and (2.2). This normalizes the properties and therefore makes it possible to compare them to samples of different sizes.

$$\epsilon = \frac{\Delta d}{d} \tag{2.1}$$

where d is the original thickness of the sample.

$$\sigma = \frac{F}{A} \tag{2.2}$$

Stress and strain can be plotted against each other, creating a stress-strain diagram, see figure 2.7.

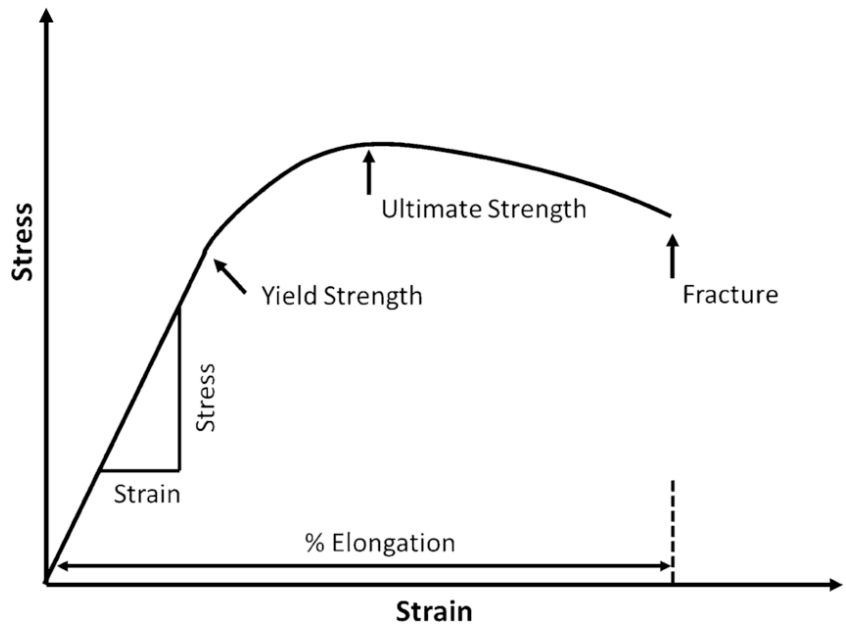

Figure 2.7: A typical stress strain diagram [27].

Young's modulus (E_s), also referred to as modulus of elasticity, describes the elastic properties of a material undergoing compression or tension in one direction [28]. The modulus is calculated through division of stress by strain in the linear elastic region, as displayed in figure 2.7. A higher value of the modulus represents a material with a higher stiffness.

While Young's modulus is measured at the instantaneous loading, the aggregate modulus (H_A) is measured when the tissue has reached equilibrium and the fluid flow has ceased. A higher aggregate modulus indicates a material that deforms less during loading [29]. To calculate the aggregate modulus using data from unconfined compression the value of Poisson's ratio (v_s) is required, see equation 2.3.

$$H_A = \frac{1 - v_s}{(1 + v_s)(1 - 2v_s)} E_s \tag{2.3}$$

Two common methods used to describe a material's viscoelastic properties are stress relaxation and creep tests. Stress relaxation measures the change in stress under a constant strain whereas creep measures how the sample strains under a constant stress, see figure 2.3. The biomechanical experiment in this study will be composed of a step-wise stress relaxation test.

Stress relaxation tests result in a stress-over-time graph with the characteristic immediate increase in stress followed by a slow decrease as the strain remains constant. When compressed, the fluid and solid matrix in the tissue start to react to the load. The initial load is mainly carried by the incompressible fluid which shifts up towards the surface and eventually seeps out. As the strain is held constant, a redistribution of the fluid takes place and the load is increasingly carried by the solid compartment until a new equilibrium is reached. This occurs when the fluid flow ceases [30].

2.4.1 Viscoelastic material model

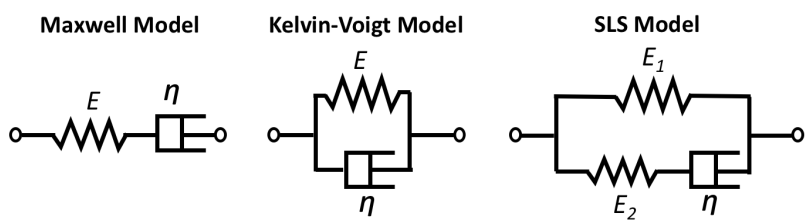

Figure 2.8: Three material models. Maxwell Model (left), Kelvin-Voigt Model (center) and SLS Model (right).

The combination of viscous and elastic material properties can most realistically be obtained through modelling. These models are most commonly created by combining two elements with different characteristics, springs and dashpots, see figure 2.8. The spring is an elastic element whereas the dashpot acts as a damping component, representing the time dependency. The Maxwell model and the Kelvin-Voigt

model are the two most basic material models, capturing stress relaxation and creep differently. The Maxwell model, consisting of a spring and a dashpot in series, is better at representing the stress relaxation response, whereas the Kelvin-Voigt model, consisting of a spring and a dashpot in parallel, better represents creep response.

These two models are often not sufficient when predicting viscoelastic material properties, instead the Standard Linear Solid (SLS) model is applied, a spring in parallel with a Maxwell model, sometimes also illustrated as a spring in series with a Kelvin-Voigt model [31]. The SLS model handles the drawbacks with the previously mentioned models and can therefore better account for creep, recovery and stress relaxation.

When further complexity is needed, springs and dashpots can be added in different combinations, resulting in an unlimited possibility of material models. The Generalized Maxwell model is the most general form of modelling viscoelastic materials. It consists of a single spring in parallel with unlimited Maxwell components, allowing it to represent the varying relaxation times found in viscoelastic tissue [31]. During stress relaxation, all Maxwell elements are exposed to equal strain and the stress experienced in each element is summed up to provide the total stress for the system, as shown in equation 2.4.

$$\sigma(t_i) = \left(E_0 + \sum_{i=1}^{M} E_i e^{-t/\tau_i} \right) \epsilon_p \qquad i = 1, 2..., M \tag{2.4}$$

The amount of Maxwell elements in parallel is represented by i, E_0 is the elastic modulus of the single spring and E_i represents the elastic modulus of the springs in the Maxwell elements. τ_i is the relaxation time constant, obtained through dividing the viscosity modulus, η_i, with the elasticity modulus, E_i. The applied strain is expressed with ϵ_p.

When constant strain is applied to the system, the instantaneous response is the extension of the springs. This can be demonstrated in equation 2.4, when t is close to zero, the stress can more or less be expressed as the sum of the elastic moduli E_0, E_1 and E_2. As time elapses, the stress from each Maxwell component is transferred to the dashpots, acting as dampers. Once the dashpots have undergone complete relaxation and as t goes to infinity, the exponential term in equation 2.4 becomes zero, leaving the single spring E_0 responsible for the equilib-

rium stress. This allows the system to be a suitable model for a solid material.

The previously mentioned SLS model can be seen as a simple Generalized Maxwell model with only one Maxwell branch. When modeling the data obtained from the biomechanical testing of the menisci, two Maxwell elements will be connected to obtain more precise material properties, see figure 2.9.

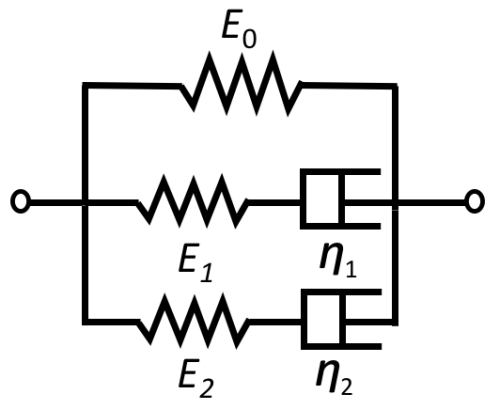

Figure 2.9: A Generalized Maxwell model with two Maxwell elements.

2.5 Current state of the art research

Discovering early stage OA in patients is a challenging task as it highly relies on radiographic findings in combination with clinical symptoms, both of which are more prevalent in late stage OA. The disease knowledge and treatment innovation in OA is considered slow, primarily due to the lack of reliable biomarkers to diagnose and assess the progression [32][2]. Studies have been made to identify differential expressions of proteins between OA and healthy samples. In knee synovial fluid, profound differences have been found in the global protein profile of controls compared to OA patients [2]. A study of the proteomics of osteoarthritic and healthy human menisci found that when comparing medial menisci, the healthy samples exhibited overall lower protein intensities [33]. The most prominent differences were identified among matrix proteins and inflammation-involved pathways [33]. Differentially expressed proteins

can potentially be used as OA biomarkers which proves the importance of further research into the proteomics of osteoarthritic tissue.

The meniscus in the arthritic knee is weakened and can therefore not function in the same manner as a healthy meniscus i.e. absorbing shocks and distributing loads across the knee. An analysis of human menisci in arthritic knees showed proof of disruption of the meniscal matrix, primarily on the posterior horn which is where the meniscus is predominantly exposed to loading during knee flexion [34]. Katsuragawa et al. [35] found that the medial meniscus is evidently more degenerated than the lateral, mostly in the body and posterior sections. Microscopy findings showed that the diameter of collagen fibrils was reduced as well as being less densely placed. Concerning the biomechanical properties of OA vs control menisci, the aggregate modulus was found to be 40% lower in the medial meniscus in arthritic knees, proving a weakened compressive capacity [35]. Tensile and indentation tests were made on 24 menisci with varying degrees of degeneration where the results showed that there is a significant decrease in compressive strength as the samples become more degenerated [36]. The tensile strength however seems unaffected by degeneration [36], supporting future research to focus on how the meniscus' compressive properties change with the progression of OA.

Chapter 3

Materials & methods

3.1 Overview of the methods

This project is composed of two different elements where the results will be combined in order to gain a greater knowledge of the subject, see figure 3.1. The project began with a proteomic experiment which focused on preparing the meniscal samples for mass spectrometry in order to analyse their protein composition. The second stage consisted of biomechanical testing of an array of menisci to evaluate material properties. The approach and methods behind both parts will be described in detail in the following sections.

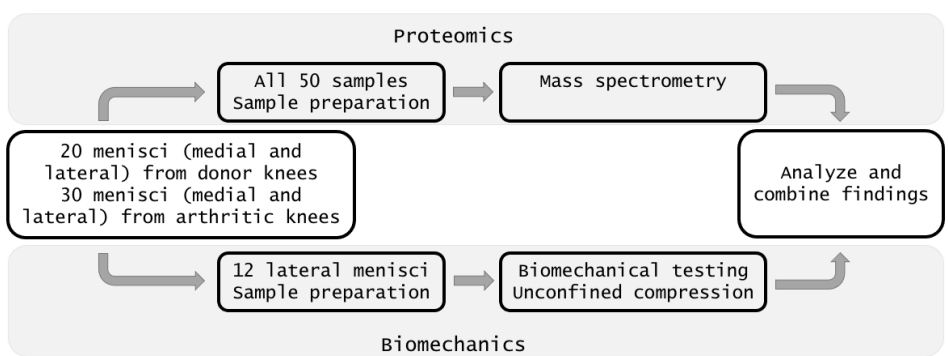

Figure 3.1: Overview of the process.

3.2 Proteomic experiment

50 menisci, both lateral and medial, from the MENIX Biobank in Lund were used. 15 knees were from patients with medial compartment end-stage knee OA, a form of OA that mostly affects the medial compartment of the knee, undergoing total knee replacement. The remaining menisci were from 10 deceased donors without known knee OA. In total there were 12 males and 13 females between the ages of 18-80 with a BMI ranging from 16.4-42.4, see table 3.1. A crude visual macroscopic grading of meniscal integrity was performed by one medical doctor, where a lower score represents a less damaged meniscus, and a higher score represents a more degenerated and torn meniscus tissue. The histological scoring was based on the grading system created by Pauli et al. [34] where grades ranging from 0-4 represents normal tissue, 5-9 indicates mild degeneration, 10-14 represents moderate degeneration and finally, 15-18 implies the most severe degeneration. The lowest and the highest score of the menisci used in this study were 3 and 18 respectively.

Plugs (Ø 4 mm) were taken on the outer third and as close to the body part as possible on the anterior half of the menisci[1], see figure 3.2 and 3.3. Before being stored in -80°C overnight, the menisci, together with their respective plugs, were photographed and documented.

Table 3.1: Properties of the menisci, mean ± SD.

Meniscus group	Score	Age	BMI [kg/m^2]
Lateral OA	12.6±2.46*	51.2±18.0	30.3±4.44
Medial OA	14.3±2.26*		
Lateral healthy	7.5±2.72	65.5±8.0	28.0±7.61
Medial healthy	9.6±1.78		

* Missing values for 5 meniscus pairs.

[1]Some of the menisci were very degenerated and plugs could therefore not be taken in the same manner as the rest. A scalpel was instead used in these cases.

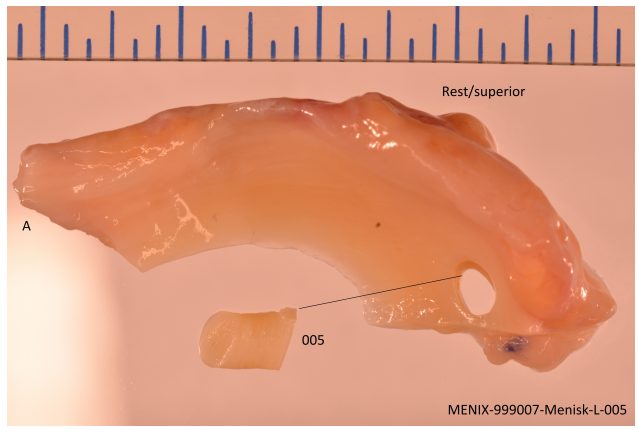

Figure 3.2: Meniscus from healthy knee.

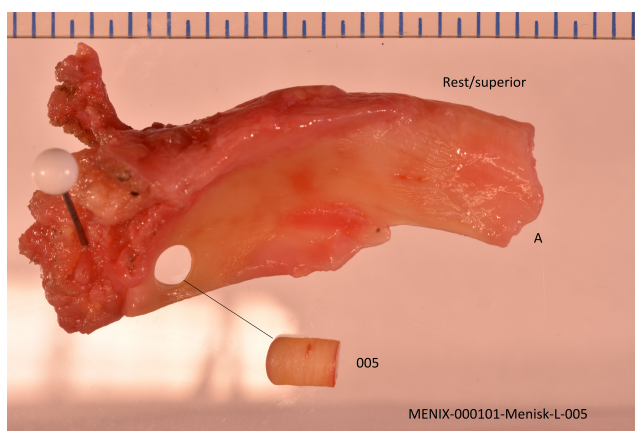

Figure 3.3: Meniscus from OA knee.

3.2.1 Pulverization

The plugs were the following day placed in eppendorf tubes with punctured lids and freeze dried for 24 hours. The plugs were then transferred into new tubes that had been weighed beforehand so that the weights of the frozen samples could be obtained. Three of the samples were selected to test the TissueLyser II (Qiagen), a metal bead was added to each tube and were then run for 2 + 3 minutes at 30Hz to assess the pulverization process. The chosen samples were the smallest plug, an average plug and the largest plug. Unfortunately the samples

did not pulverize, so, before proceeding with the rest of the samples, 15 ml/mg of extraction buffer 1 (combination of Guanidine hydrochloride (GuHCl), anhydrous sodium acetate (NaAc),6-aminocaproic acid and benzamidine hydrochloride hydrate) and 5 mM N-Ethylmaleimide (NEM) were added to the three samples prior to an additional 2 minutes at 30Hz eLyser results were still not satisfactory so the decision was made to further freeze dry all the samples for an additional 24 hours.

The samples were subjected to several rounds of 2-3 minutes at 30Hz in the TissueLyser as well as soaking in 15 ml/mg of extraction buffer 1 + NEM. An additional 200µl of the solution was added to each sample before centrifugation and storage in -80°C over night.

3.2.2 Extraction

The metal beads were removed and rinsed off with 200µl of the solution (extraction buffer 1 + NEM) which was collected in each tube. The tubes were then centrifuged for 30 minutes at 4°C at 13200 rpm. This resulted in each sample separating into a pellet and supernatant. As much of the supernatant as possible was collected from each tube and saved in new ones (extraction 1). Parafilm was placed on the tubes with the pellets and punctured with small holes to prepare them for the freeze dryer where they were left for 24 hours after being in the -80°C freezer overnight.

Protein quantification (Pierce BCA Protein Assay Kit from ThermoFischer Scientific) was carried out to determine the approximate amount of protein in the supernatant. Metal beads were then added in the tubes with the pellets and run in the TissueLyser for 2 minutes at 30 Hz. 110µl of the solution was added to all the tubes except for the smallest pellet which only required 60µl. The pellets were TissueLysed for another round of 2 minutes at 30 Hz and then filled up with the solution until they contained 15 ml/mg relative to the initial weight. The metal beads were, in the same manner as previous, removed and rinsed with 200µl of the solution. The samples were then put in the refrigerator on a shaker. The following day the samples were centrifuged for 30 minutes at 4°C and 13200 rpm and the supernatant could then be removed and put into new tubes (extraction 2). To obtain the third extraction the pellets were once again filled up with extraction buffer 1 and NEM until

a concentration of 15ml/mg was reached and then soaked for 24 hours. They were centrifuged and the supernatant was removed in the same way as previously mentioned (extraction 3).

The three extractions from each meniscal plug were pooled together as well as creating four new samples to function as the MS-library. These were produced by collecting 100µl from each sample belonging to the following categories: patient medial meniscus (MY), patient lateral meniscus (LY), donor medial meniscus (MG) and donor lateral meniscus (LG). The 54 samples were then put in the SpeedVac (ThermoFischer Scientific) and evaporated until sufficiently dried.

3.2.3 Sample preparation

To prepare the samples for MS, several steps of sample preparation were performed. 500µl of 0,1M ammonium bicarbonate (AMBIC) (pH-regulated to 7,4) was added to each of the samples to dissolve the pellets. In order to break the SS-bonds, 10µl of 4mM dithiothreitol (DTT) was added to each sample followed by 30 minutes on a shaker at 56°C. The samples were then alkylated with 20µl 16 mM iodoacetamide (IAA) for 1 hour in the dark at room temperature. The samples were then evaporated in a SpeedVac until dry for approximately 5 hours. 100µl of 0,1M AMBIC and 900µl of ethanol was added to the extracts before being placed on a shaker at 4°C overnight. After precipitation, the next steps were centrifugation at 13200 rpm for 1 hour at 4°C, following the removal of 900µl supernatant. The samples were then suspended in 500µl of 0,1M AMBIC for 1 hour at 37°C. The largest lumps of the sample were atomized with a pipette tip and the samples were put in the refrigerator over the weekend.

Due to the samples not dissolving properly, they were treated with a low concentration of Trypsin Gold (MS grade), 200µg in 400µl AMBIC was evenly distributed over the 54 samples, vortexed and incubated for 24 hours at 37°C. 1 ml Milii-Q water was added to each sample and spin filters (0,22µm pore size) were used to remove the largest particles in each sample in order to facilitate for the upcoming 30kDa-filtration. Through several 10-minute rounds of 10000 rpm, all the samples were filtered and the clear solution accumulated at the bottom was collected and transferred into new tubes.

The Pierce Quantitative Colorimetric Peptide Assay from ThermoFischer Scientific was used to determine the peptide concentrations in each sample. Since the obtained results were high, calculations were made for each sample in order to decide to which level they should be diluted to achieve satisfactory concentrations. To obtain 350µg of protein from every sample, different volumes were extracted from each and filled up with Milli-Q water to balance the volumes. 400µg of trypsin diluted in 800µl of 0.1M AMBIC was divided equally into all samples followed by incubation over night at 37°C on a shaker.

30 kDa-filtration

The samples were dried in the SpeedVac, and then dissolved in 100 µl 1M NaCl/0.1% FA+100 µl Milli-Q water. To filter the samples further, 30 kDa filtration was performed, using a 30 kDa filter (Pall Corporation, 96 well) together with a vacuum pump (Rocker 400, VacMaster VCU). The 30 kDa filter was conditioned with 200 µl 0.5 M NaCl/0.1% formic acid (FA), the samples were then added and finally, the filters were washed with 80 µl 0.5 M NaCl/0.1% FA. To determine the remaining peptide concentration, peptide quantification was performed with Pierce Quantitative Colorimetric Peptide Assay.

C18

To desalt the samples a C18 cleanup was performed. This was done using the AssayMAP Bravo platform (Agilent Technologies, Santa Clara) robot and C18 columns (Agilent Technologies), each being able to bind 100 µg of protein. Based on the result from the peptide quantification a volume containing 110 µg of protein was used from each sample. For sample 256M a volume corresponding to 110 µg was not available. All available samples were used, which corresponded to approximately 73 µg. The sample volumes were then adjusted with 0.1% FA to reach 320 µl. 90% ACN/0.1% FA was used as priming buffer, 0.1% FA was used as equilibration buffer and 80% ACN/0.1% FA was used as elution buffer.

High pH reversed phase fractionation

The pooled samples were fractionated (high pH reversed phase) using the AssayMAP Bravo platform and the same C18 columns as for the C18

cleanup. The volume containing 110 µg for each sample was transferred into a tube and dried in the SpeedVac. The samples were then dissolved in 280 µl 200 mM ammonium formate (AF) with pH 10. 90% ACN was used as priming buffer and 20 mM AF, pH 10, was used as equilibration buffer. The samples were eluted in 6 fractions using elution buffers containing 4, 10, 15, 20, 25 and 80% ACN together with 20mM AF respectively. All the samples were dried in the SpeedVac, and then resuspended in 50 µl 0.1% FA. Peptide quantification was performed with Pierce Quantitative Colorimetric Peptide Assay.

3.2.4 Mass spectrometry

Mass spectrometry was performed to identify the proteins in the samples. The samples were randomly analysed with an EASY-nLC 1000 (Thermo Scientific) coupled to a Thermo Scientific Q-Exactive HFX™ mass spectrometer using data-independent acquisition (DIA). For LC, mobile phase A consisted of water containing 0.1% FA and mobile phase B consisted of ACN containing 0.1% FA. Peptides were loaded on an Acclaim PepMap® 100 nanoViper pre-column (Thermo Scientific, C18, 3 µm particles, 75 µm i.d. 2 cm long) at 5 µL/min mobile phase A. The peptides were separated on a PepMap® RSLC C18 analytical column (Thermo Scientific, C18, 2 µm particles, 75 µm i.d. 25 cm long) at 300 nL/min using an ACN/formic acid gradient consisting of an initial step of 3–7% B over 5 min followed by 7–20% B over 85 min, 20–30% B over 20 min, 30–90% B over 5 min, held at 90% B for 5 min and then equilibrated for 15 min at 3% B. Separation was performed at 45°C and the total acquisition time was 125 min. The DIA and DDA settings are presented in the appendix.

The MS raw data were further analysed with Spectronaut™Pulsar software for protein identification and quantitative data extraction. The human protein fasta files were downloaded from the UniProt database (210210). Default settings were used with additional modifications: cysteine carbamidomethylation was used as a fixed modification, and deamination, pyro-glutamic acid (N-term Glu to pyroglutamic acid), methionine oxidation, hydroxyproline and acetylation were used as variable modifications. Using Trypsin/P as the specific digestion type with maximum of 2 miss cleavages. A subsequent protein search was conducted in Spectronaut™ Pulsar using the recently created spectral library and

the same human database as background proteome. Precursor quantitation was performed at MS2 level, and area under the curve was used for quantitation.

3.2.5 Data analysis of the proteomic data

The data acquired from the MS was plotted and analysed in R and the program Proteomill. From Proteomill, the protein levels from each sample could be calculated and with R, a principal component analysis (PCA) plot, a heatmap and the protein regulation were obtained.

PCA is a useful tool when analysing datasets that are multidimensional, i.e. have several measurements for each sample. PCA increases the interpretability of datasets while keeping as much information as possible by reducing the amount of dimensions. The dataset is represented with a covariance matrix where eigenvectors and eigenvalues can be calculated. The eigenvectors with the highest corresponding eigenvalues are selected and used as new basis vectors onto which the dataset is projected. The amount of eigenvectors used, also called principal components, determines how much of the variability in the dataset that can be explained. In this case, two principal components were used, scaling down the original amount of dimensions to a 2D plot. Unsupervised clustering was implemented to assess the grouping of the four categories MG, MY, LG and LY.

The heatmap compares the relationship of the protein levels between all samples. A similar relationship of protein levels in two samples will mark the cell in the intersection between these two samples in a color representing a value close to one. However, the comparison only takes the protein distribution into consideration, and not the actual values of the protein levels. It is therefore important to keep in mind that a correlation close to one does not directly imply that the samples are close to identical in regards to the actual protein levels. Dendrograms were also used to further visualize the clustering of the samples.

In all plots the limit of missing values was set to 2, meaning that all proteins with more than 2 missing values were excluded from the calculations.

3.3 Biomechanical testing

The second approach of the project included mechanical testing of the menisci. For this part, 8 mm punches were taken from the previously used menisci in the cases where enough tissue remained, these samples are presented in table 3.2 and 3.3. On these plugs, unconfined compression was performed in order to obtain mechanical propetries for each sample. Poisson's ratio was determined through literature research.

Table 3.2: Properties of the donor menisci used for the mechanical testing. The height refers to the thickness of the punch.

Sample	Height [mm]	Score	Age	BMI [kg/m^2]	Gender
007L	4	9	52	26.78	M
008L	5	3	31	22.84	F
009L	3.2	6	61	23.31	F
014L	4.4	7	58	33.24	M
090L	3.5	7	43	42.43	M
092L	3.5	6	50	34.22	M
Mean±SD	-	6.3±1.8	49.2±10	30.5±6,9	-

Table 3.3: Properties of the patient menisci used for the mechanical testing. The height refers to the thickness of the punch.

Sample	Height [mm]	Score	Age	BMI [kg/m^2]	Gender
101L	4	14	72	28.73	M
139L	3.5	12	65	27.47	M
140L	4	-	66	35.5	F
256L	3.5	-	72	34.98	M
316L	3.2	17	76	28.73	M
366L	3.5	13	51	37.38	F
Mean±SD	-	14±1,9	67±8,1	32.1±3,9	-

3.3.1 Sample preparation

The menisci were first thawed in room temperature and then, using biopsy punches, 8mm plugs were taken from each meniscus and kept hydrated in PBS prior to testing. Due to the slanted shape of the meniscus, each plug was carefully cut with a scalpel to create parallel

edges. The cut was always made on the femoral side. The plugs were then photographed together with their respective meniscus, see figure 3.4 and 3.5. Using a digital caliper, the thickness of each sample was determined.

Figure 3.4: Lateral menisci from donor knee together with the intact 8 mm punch.

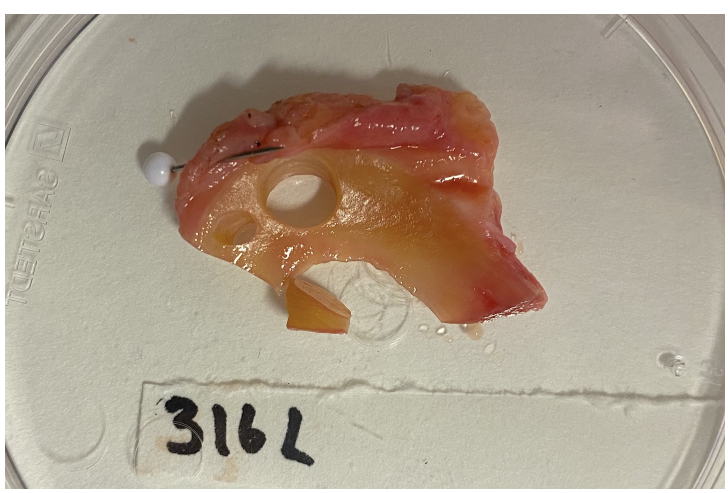

Figure 3.5: Lateral menisci from osteoarthritic knee together with the intact 8 mm punch.

3.3.2 Experimental design

An Instron 8511.20 was used for the testing of the meniscus with a load cell of 250N and a 10mm compressive tip, see figure 3.6. To ensure the samples were kept moist during the tests a chamber was 3D-printed in polyoxymethylene (POM), see figure 3.7. In the chamber, the samples were fixed on the cut side down with a drop of superglue and then filled with PBS to maintain hydration.

Figure 3.6: Instron set-up with chamber and sample.

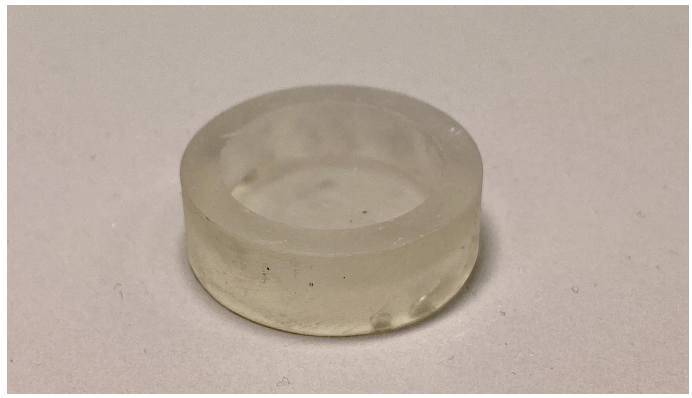

Figure 3.7: 3D-printed chamber.

All samples were equilibrated with a pre-load of 0.3 N for 10 s. Four cycles of step-wise stress relaxation was performed, each step involving a 5% increase in displacement relative the sample's initial thickness with a velocity of 0.5 mm/s. The holding time, i.e. the amount of time the displacement was held, was 200, 300, 400 and 500 seconds respectively for the four steps, see figure 3.8.

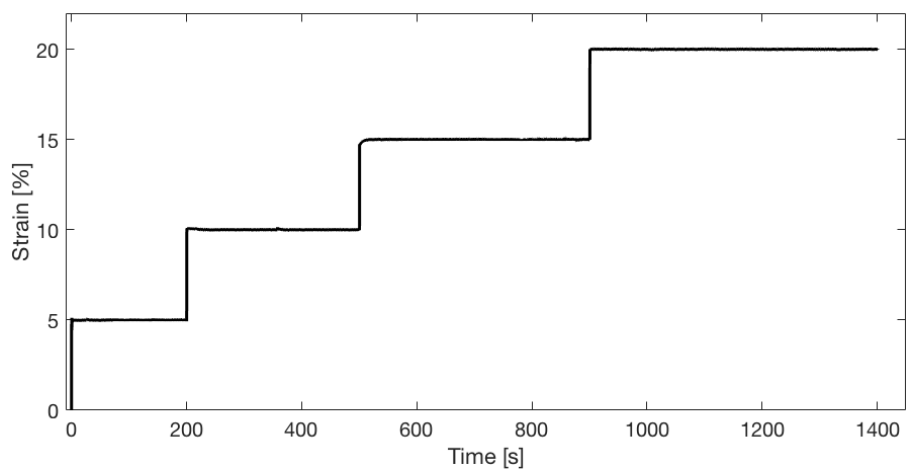

Figure 3.8: The applied strain for the samples during the unconfined compression test.

3.3.3 Data analysis of the biomechanical data

The data acquired from the biomechanical experiment (force, time and displacement) was exported to Matlab where the results were plotted and analysed. Due to high noise levels, the data was smoothed with 13 values before and after the highest force values.

Young's modulus, E_s, was then calculated through the linear region of the stress-strain curve between 70% and 90% strain for each peak. To visually assure that the modulus was representative for each peak, the slope was plotted in the stress-strain diagram for each peak. The relaxation ratio was obtained by measuring how much, in percent, the stress relaxed compared to its start value after the holding time (200, 300, 400 and 500 sec). The relaxation time was measured when the tissue relaxed less than 150 Pa/min. Finally, the aggregate modulus was calculated from equation 2.3 where Poisson's ratio, v_s, was set to 0.45 [37].

Generalized Maxwell model

To further analyse the acquired biomechanical data, peak 2, 3 and 4 from every sample were fitted to a Generalized Maxwell model using Matlab. This gave us the parameter values for E_0, E_1, E_2, τ_1 and τ_2. The first peak was not included due to a too high pre-load without sufficient relaxation. By smoothing the data with 5 values and through optimization, the data was fitted to the Generalized Maxwell model with one spring and two parallel branches consisting of a spring and a dashpot in series, see figure 2.9. The force equation for this type of model is shown in equation 3.1 where ε_p is the applied strain which in every case was 0.05.

$$\sigma(t) = E_0\varepsilon_p + \varepsilon_p\Big(E_1 e^{-t/\tau_1}\Big) + \varepsilon_p\Big(E_2 e^{-t/\tau_2}\Big) \tag{3.1}$$

$$\tau_i = \eta_i/E_i \qquad i = 1, 2 \tag{3.2}$$

The parameters obtained from this fitting were E_0, E_1, E_2 τ_1 and τ_2.

Chapter 4

Results

4.1 Proteomic results

A total of 1076 proteins were identified in the 50 meniscal samples. Just over half of the proteins were dismissed after removing proteins with a missing value greater than two, leaving 517 eligible for the analysis.

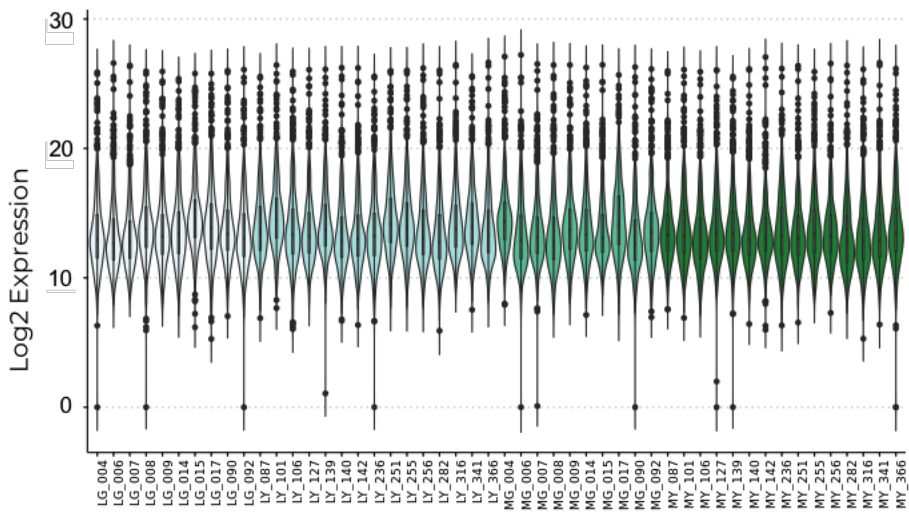

Figure 4.1: The total protein expression for each meniscal sample.

Figure 4.1 is a violin plot representing the total dynamic protein range for each sample. A similar representation is shown in figure 4.2 where the 50 menisci are sorted into 4 groups, lateral healthy and OA as well as medial healthy and OA.

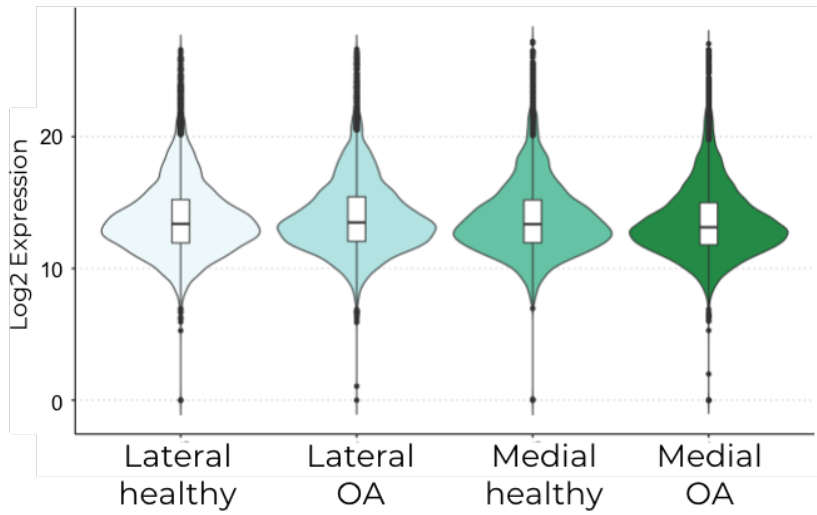

Figure 4.2: The total protein expression for each group of menisci.

To examine the protein regulation in menisci from healthy and arthritic knees, both lateral and medial menisci were compared to each other in the two groups. The total result of the up and down regulated proteins are shown in figure 7.1 in the appendix. In figure 4.3 and 4.4, the up and down regulation of proteins with the highest and lowest fold change can be seen between LY and LG as well as MY and MG respectively.The fold change shows the protein ratio of meniscus from osteoarthritic knee with respect to healthy knee. The colour combination green and grey represents the comparison between medial menisci whereas blue and black represent the lateral menisci. The bars in the graph represent a 95% confidence interval and implies the significance of each comparison. If a bar should cross the center line it signifies that no difference could be found, this applies to the grey and black bars. This ultimately means that the blue bars represent the proteins in which a fold change between healthy and arthritic knee lateral menisci has been detected and green bars represent the proteins in which a fold change between healthy and arthritic knee medial menisci has been detected.

In order to decrease the probability of confounding, the data has been adjusted for age, BMI and sex so that these factors have minimal influence when comparing differences in protein abundance.

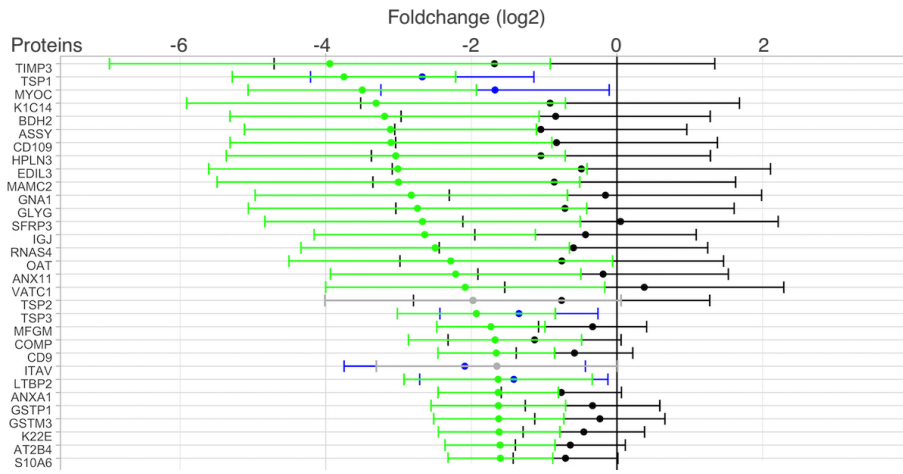

Figure 4.3: The most down-regulated proteins in meniscus from OA knees compare to healthy knees. Green and grey represents medial menisci while blue and black represents lateral menisci.

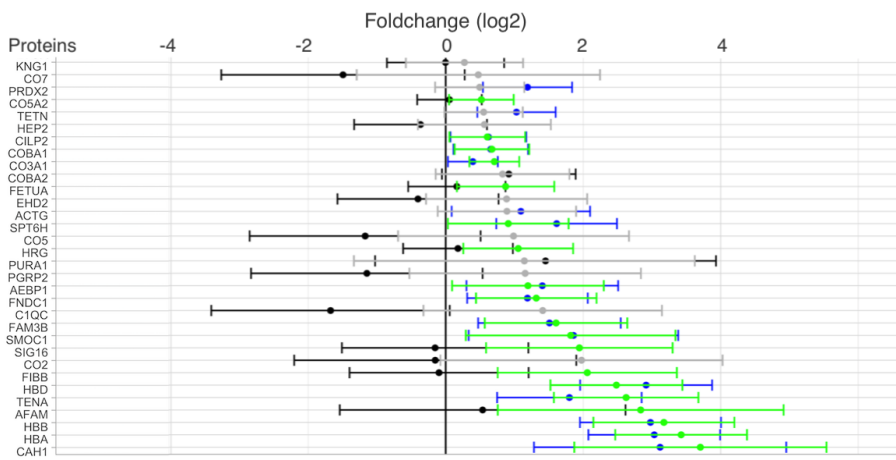

Figure 4.4: The most up-regulated proteins in meniscus from OA knees compare to healthy knees. Green and grey represents medial menisci while blue and black represents lateral menisci.

A total of 168 proteins were found to be significant in any of the comparisons between OA vs healthy and lateral vs medial menisci. Of these, 111 proteins had a statistically significant fold change between medial healthy and medial OA-knee, 19 of which had a higher intensity in healthy menisci. 32 proteins were found to have a significant fold change between lateral healthy and lateral OA-knee, whereof 16 exhibited higher intensities in healthy meniscus.

The two most significantly *down-regulated* proteins in both medial and lateral arthritic knees were TSP1, thrombospondin 1, (medial(-3.75 [-5.28, -2.22]), lateral (-2.67 [-4.21, -1.14])) and MYOC, myocilin, (medial (-3.5 [-5.07, -1.93]), lateral (-1.67 [-3.24, -0.11])). Both are glycoproteins involved in cell-to-cell and cell-to-matrix interactions.

The most significantly *up-regulated* proteins in both medial and lateral OA-knees were HBA, hemoglobin A, (medial (3.42 [2.47, 4.38]), lateral (3.03 [2.07, 3.99])), HBB, hemoglobin B, (medial (3.17 [2.15, 4.20]), lateral (2.98 [1.95, 4.00])) and CAH1, carbonic anhydrase 1, (medial (3.70 [1.87, 5.54]) , lateral (3.12 [1.28, 4.95])). HBA and HBB are proteins involved in oxygen transportation from the lungs to tissues while CAH1 is involved in the physiological activities of calcification and mineralization [38].

The overall highest fold change is found with the protein TIMP3, metallopeptidase inhibitor 3, where the intensity in arthritic medial knee is down-regulated with a factor of '3.94' [-6.97, -0.92] in relation to healthy medial menisci. Both proteins CO3A1, collagen type III, and CILP2, cartilage intermediate layer protein 2, are up-regulated in medial and lateral arthritic knee with a fold change of medial (0.71)[0.34, 1.07], lateral (0.39)[0.03, 0.76] and medial (0.60)[0.05, 1.55], lateral (0.62) [0.07, 1.17] respectively. TIMP3 is a protein that inhibits peptidases involved in degradation of the extracellular matrix, CO3A1 occurs in most soft connective tissues and CILP2 is a protein that may play a role in cartilage scaffolding.

Unsupervised clustering was used for the principal component analysis (PCA) to evaluate and group the samples' proteomic identities, the results are shown in figure 4.5. The PCA-plot was created using two principal components, Dim1 and Dim2 with the variabilities 14.9% and 9.9% respectively. These values represent the share of the protein content that has contributed to the the clustering of the four groups LG, LY, MG and MY.

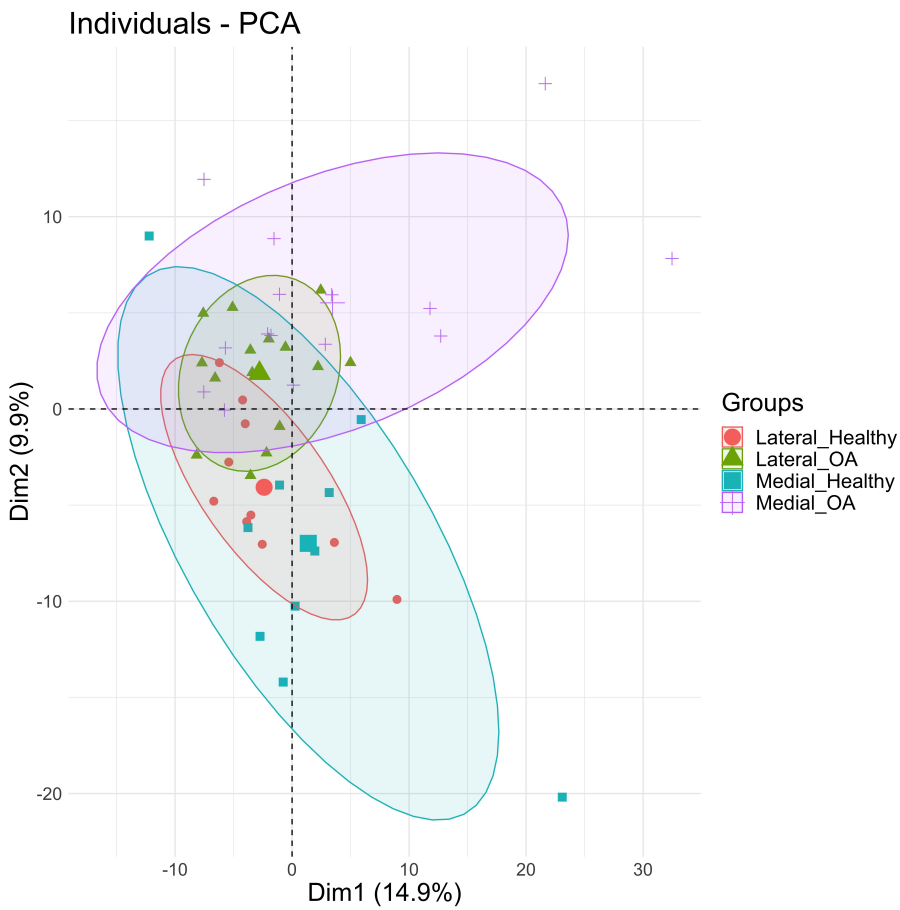

Figure 4.5: PCA-plot of meniscal samples with unsupervised clustering using two principal components, Dim1 and Dim2. The larger markers for each group represents the centre point of each cluster.

Figure 4.6 is a visualisation of the correlation between the quantitative data of each sample. The magnitude of correlation is represented in the scale to the right where the metadata (age, sex and BMI) are also included.

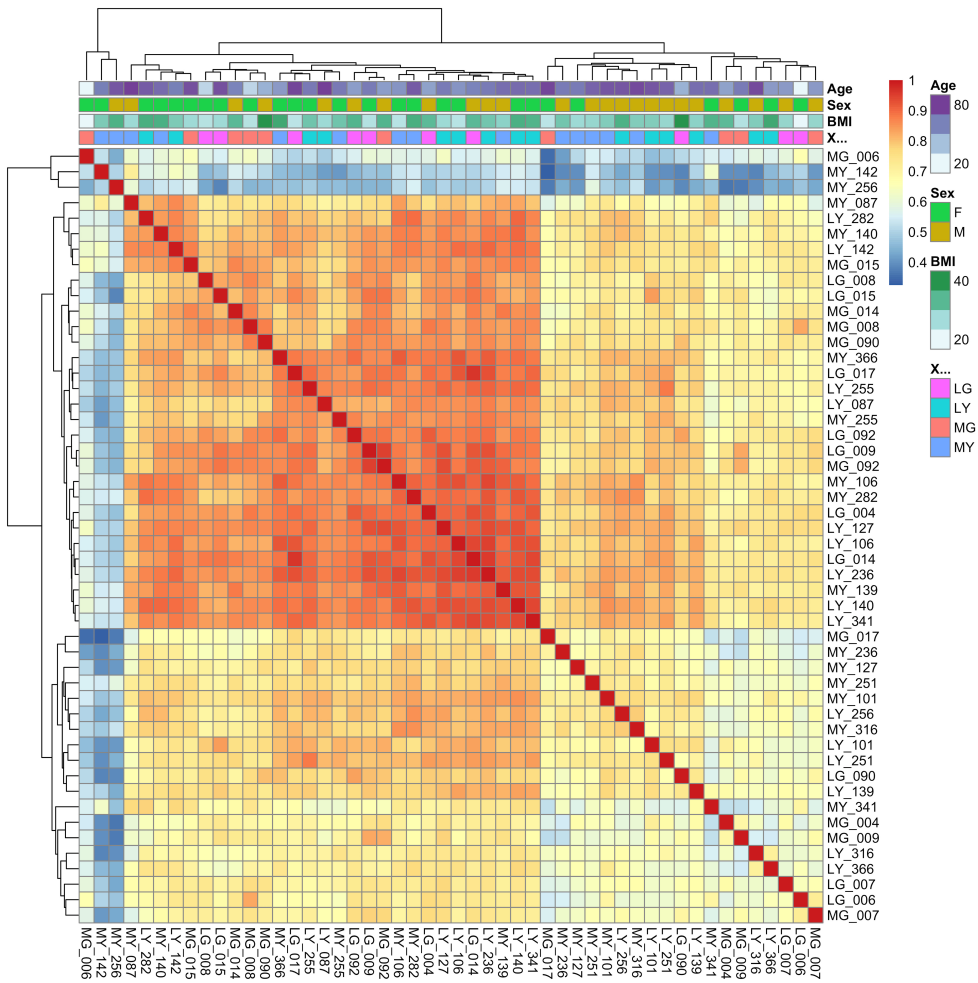

Figure 4.6: A heatmap of the sample correlation for the protein content between each sample. Red corresponds to a very similar distribution of the protein content between samples while blue corresponds to a low similarity.

4.2 Biomechanical results

In figure 4.7 force and displacement are displayed over time during the biomechanical test.

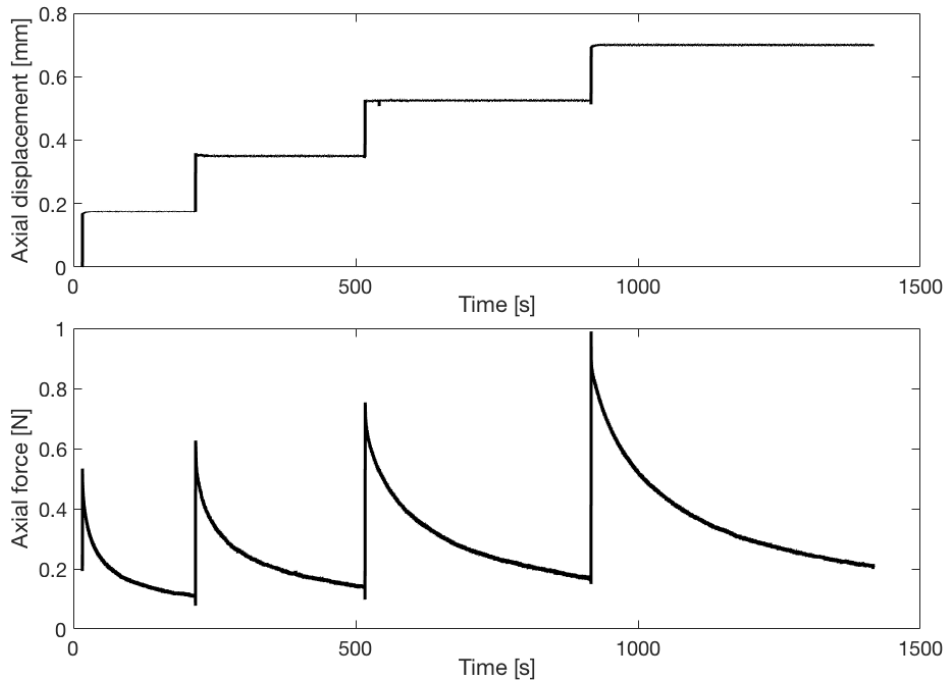

Figure 4.7: The displacement protocol and force time diagram for sample 256L.

The biomechanical properties of menisci from healthy knees and arthritic knees are shown in table 4.1 and 4.2.

Table 4.1: Calculated material parameters (mean±SD) from donor meniscus samples (n=6).

	E_S [MPa]	H_a [MPa]	Relax ratio
Peak 1	0.21±0.042	0.80±0.16	103%±7.8%
Peak 2	0.29±0.061	1.08±0.23	94%±4.7%
Peak 3	0.37±0.092	1.40±0.35	91%±7.2%
Peak 4*	0.43±0.086	1.64±0.33	92%±2.6%

* Two samples (008L and 092L) were interrupted by the instrument after three loading cycles resulting in only four samples undergoing peak 4.

Table 4.2: Calculated material parameters (mean±SD) from patient (OA) meniscus samples (n=6).

	E_S [MPa]	H_a [MPa]	Relax ratio
Peak 1	0.18±0.039	0.70±0.15	98%±8.7%
Peak 2	0.30±0.067	1.26±0.25	90%±4.4%
Peak 3	0.35±0.092	1.33±0.34	88%±4.9%
Peak 4	0.46±0.125	1.74±0.47	92%±3.9%

The stress-strain diagram, together with Young's modulus (red line) calculated at 70%-90% strain, is shown in figure 4.8

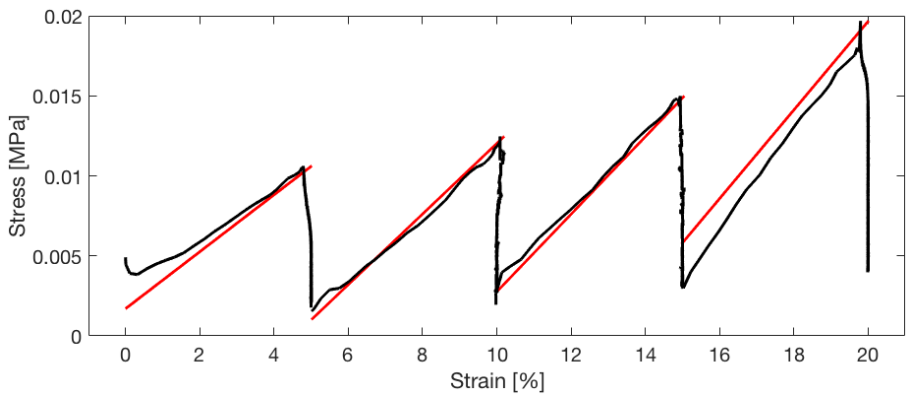

Figure 4.8: Stress-strain diagram for sample 256L. The red line represents Young's modulus at 70%-90% strain for each peak.

Further visualisation of Young's modulus for the menisci from healthy and osteoarthritic knees are shown in the box plot in figure 4.9.

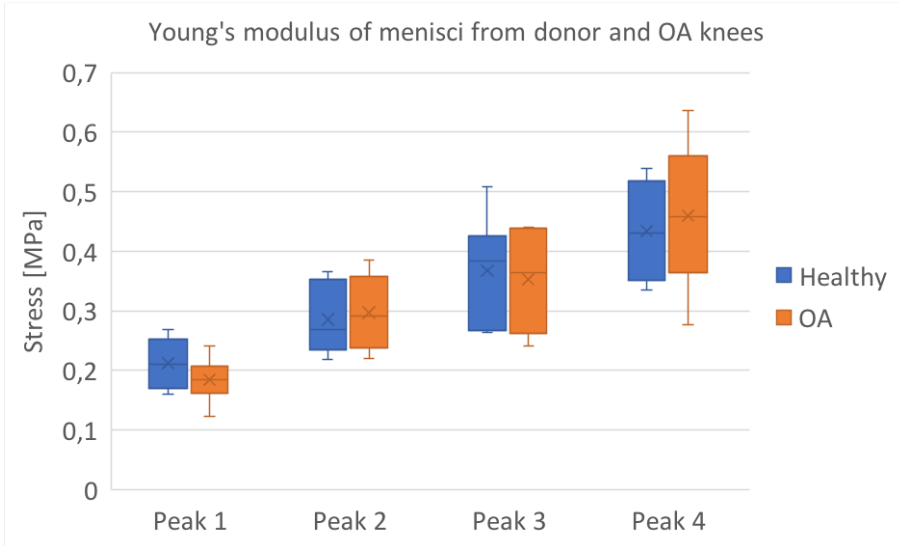

Figure 4.9: Box plot of Young's modulus of menisci from healthy and OA knees. Each box represents the values between the lower and upper quartile with the center line as the median. The whiskers represent the minimum and maximum values.

4.2.1 Material modelling

Using the Generalized Maxwell model, the model fitting parameters E_0, E_1, E_2, τ_1 and τ_2 were obtained, the values for these at peaks 2, 3 and 4 are illustrated in figures 4.10 - 4.14. The fitting of two relaxation curves are presented in figure 4.15 and 4.16.

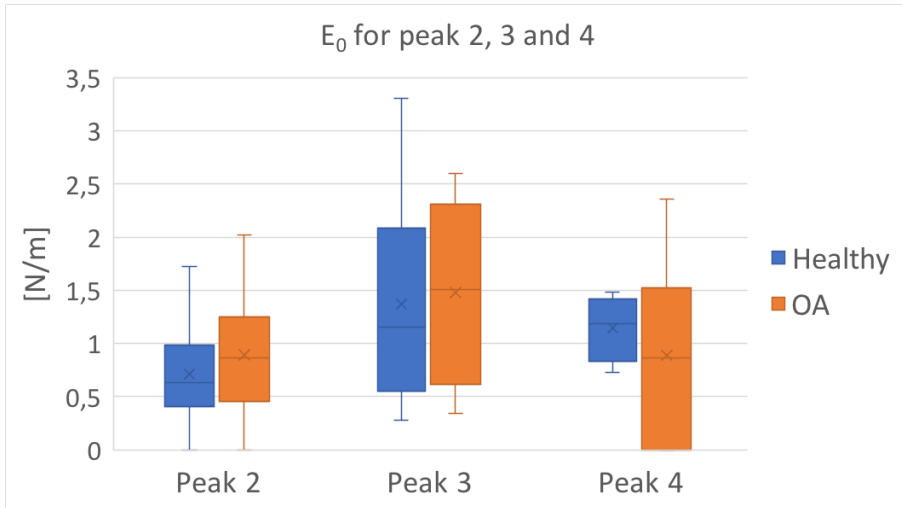

Figure 4.10: E_0 for peak 2, 3 and 4. Each box represents the values between the lower and upper quartile with the center line as the median. The whiskers represent the minimum and maximum values.

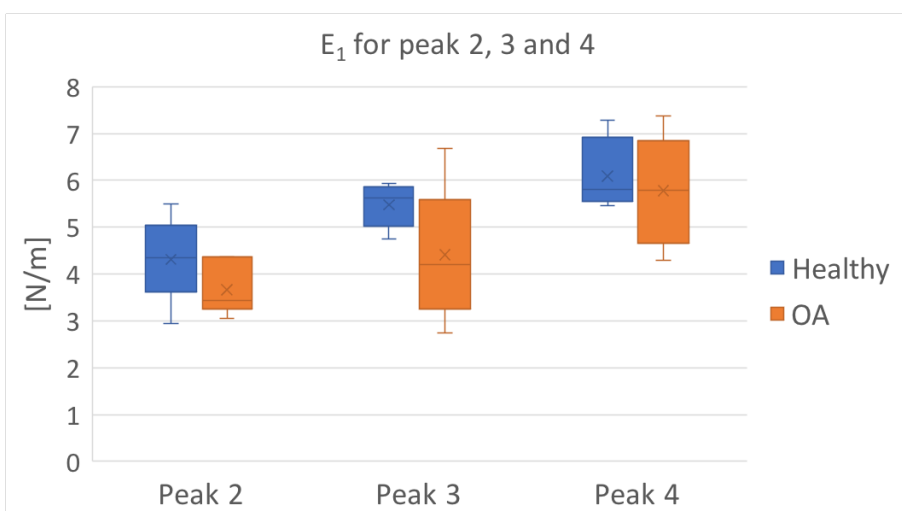

Figure 4.11: E_1 for peak 2, 3 and 4. Each box represents the values between the lower and upper quartile with the center line as the median. The whiskers represent the minimum and maximum values.

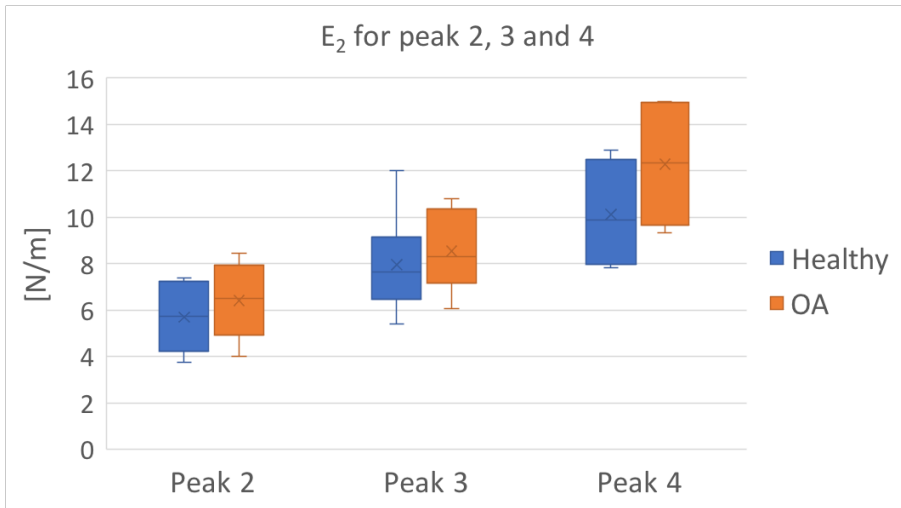

Figure 4.12: E_2 for peak 2, 3 and 4. Each box represents the values between the lower and upper quartile with the center line as the median. The whiskers represent the minimum and maximum values.

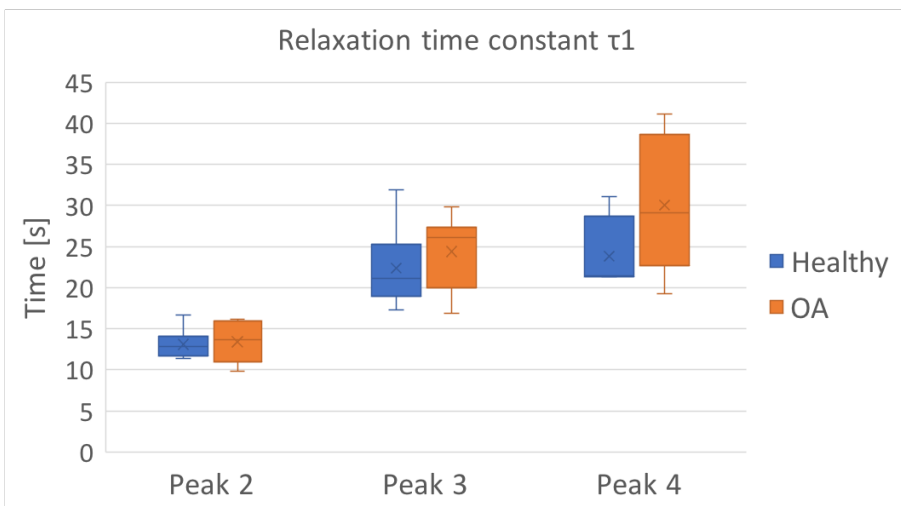

Figure 4.13: The relaxation time constant, τ_1, for peak 2, 3 and 4. Each box represents the values between the lower and upper quartile with the center line as the median. The whiskers represent the minimum and maximum values.

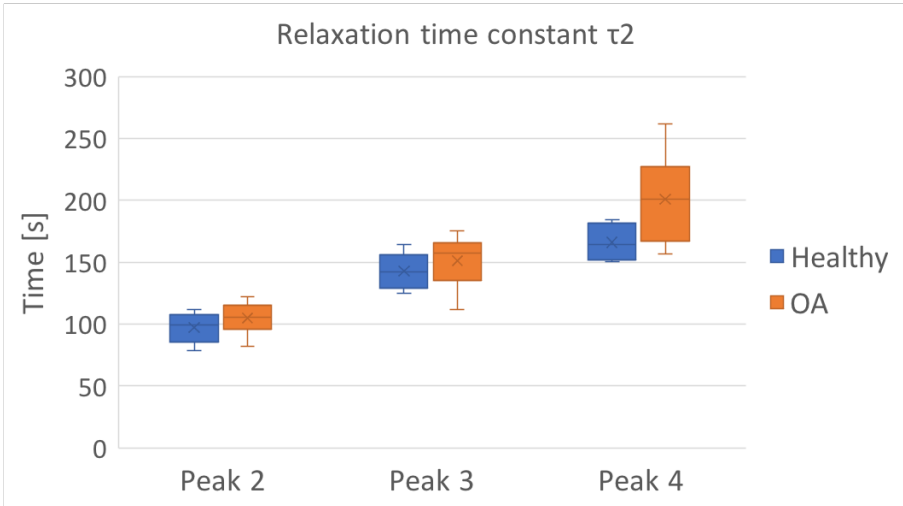

Figure 4.14: The relaxation time constant, τ_2, for peak 2, 3 and 4. Each box represents the values between the lower and upper quartile with the center line as the median. The whiskers represent the minimum and maximum values.

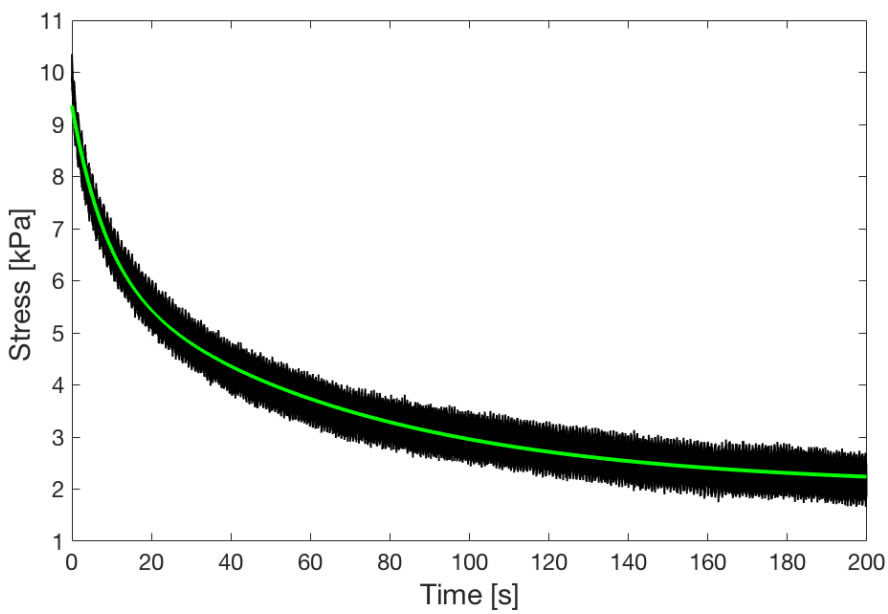

Figure 4.15: The relaxation of peak 1 from sample 256L with the curve fit from the Generalized Maxwell model.

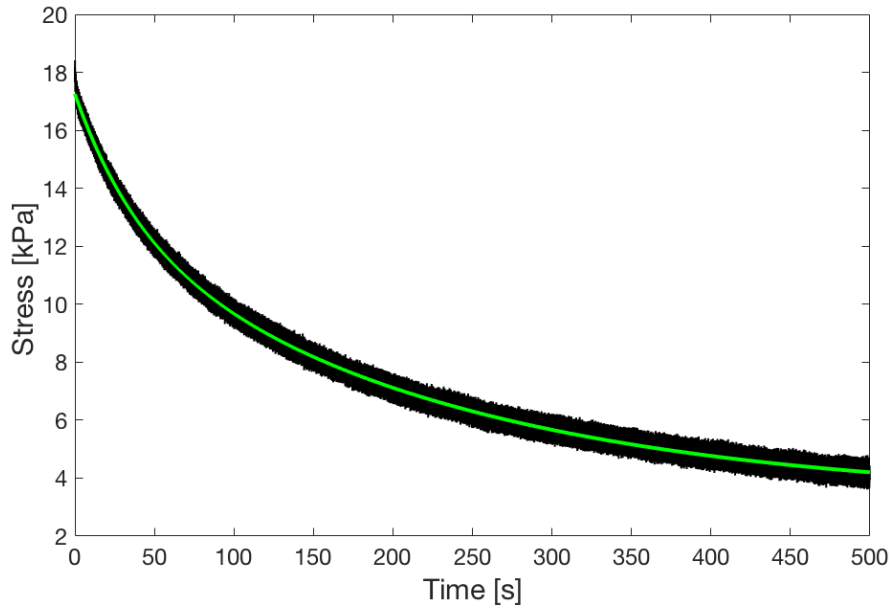

Figure 4.16: The relaxation of peak 4 from sample 256L with the curve fit from the Generalized Maxwell model.

Chapter 5

Discussion

5.1 Proteomics

The proteomic results show that the protein level is even for all samples, confirming that the sample preparation was executed in a correct manner.

The unsupervised PCA plot shows the differences in protein content between the four categories MG, MY, LG and LY. The result is shown in figure 4.5 where it is clear that the two main separations are found between medial menisci from healthy and arthritic knees. Lateral menisci from healthy and arthritic knees also exhibit some form of separate clustering but not to the same extent. From this analysis we can draw the conclusion that the protein content is most disparate between healthy and arthritic medial menisci.

5.1.1 Protein regulation

In figure 7.1 in the appendix all the up and down regulated proteins are presented. The proteins with the highest and lowest foldchanges are presented in figure 4.3 and 4.4. As mentioned in the background, the medial meniscus is often more damaged than the lateral in OA, which could be an explanation to why the protein difference is more substantial in the medial menisci.

Overall, a down regulation of glycoproteins as well as proteins involved in cell-to-cell and cell-to-matrix interactions could be seen in the menisci

from osteoarthritic knees in relation to control menisci. These findings correspond with the physiological changes that cartilage tissue undergoes during degeneration. The cartilage in menisci is, apart from water, mainly comprised of ECM where collagen and proteoglycans with GAG-chains play important roles in the matrix's structural function. Proteoglycans, a type of glycoprotein, together with their attached GAG:s, absorb water and therefor provide support during compression [39]. An example of a proteoglycan in menisci is decorin (PGS2), which was down regulated with in medial menisci from osteoarthritic knees. Adhesion glycoproteins function as the connection between cells and the matrix, making them an essential component of the ECM [39]. Thrombospondin (TSP) is one of the main adhesive glycoproteins in human meniscus, both TSP1 and TSP3 were found to be expressed less in medial and lateral menisci from arthritic knees in comparison to healthy. Studies have shown that TSP1 null mice demonstrate delayed wound healing as well as a decrease in collagen content which coincides with our results where TSP1 was the most significantly down-regulated protein. [40]

Menisci from arthritic knees, both medial and lateral, exhibited low levels of the glycoprotein myocilin (MYOC), complying with previous proteomic studies where myocilin is expressed to a greater extent in healthy controls, suggesting myocilin as a target for improving bone formation and regeneration [41].

The most significantly up-regulated protein for both medial an lateral menisci from arthritic knees is carbonic anhydrase 1 (CAH1). Overexpression of CAH1 in the synovial tissues of patients with ankylosing spondylitis, a type of arthritis, has been shown to promote improper calcification and bone resorption [38] and could therefore potentially be linked to the disease progression of OA.

Another protein that was up-regulated in both lateral and medial meniscus from arthritic knee is the collagen type III, alpha 1 protein (CO3A1). Collagen type III has previously been reported to decrease with increasing degeneration of the meniscus [42] which contradicts our result. On the other hand, meniscal tears are common in OA, explaining the need for a higher activity of extracellular matrix protein involved in repair mechanisms [5]. Murphy et al. also states that menisci from OA knees

has a higher procollagen type III content in the anterior horns compared to healthy menisci [5]. The anterior part of the meniscus was also the section that was used in our experiment.

Hemoglobin proteins HBA and HBB both exhibited higher intensities in menisci from arthritic knees which is an interesting result since low levels of hemoglobin are associated with disability and articular damage in other forms of arthritis [43]. A possible explanation to why the osteoarthritic knee menisci contain higher levels could be the tissue damage and degeneration causing internal bleeding. Cartilage Intermediate Layer Protein 2 (CILP2) was also up regulated in medial and lateral menisci, which confirms previous studies showing increased levels of CILP2 in joint diseases such as OA [44].

The heatmap seen in figure 4.6 shows the correlation between all the samples. There is no distinct correlation between the groups relating to age, sex, BMI or sample group but there is however some correlation between certain samples. The first observation is the distinction of samples 006M, 142M and 256M where 006 was a healthy meniscus while 142 and 256 were taken from OA-patients. These samples do not correlate with any of the other samples, nor with each other. From pictures and notes taken during sample extraction, it is clear that sample 256M was very damaged, forcing us to use a scalpel instead of a punch. This resulted in the sample not solely consisting of meniscus tissue which could be an explanation to the deviating result. For sample 142M and 006M nothing specific was noticed during the sample preparation.

Other samples that gave rise to some sort of clustering are samples 366M to 341L as seen in the heatmap. Six of these samples were medial and 12 were lateral, 12 were from patients and six were from donors, 11 were female and 7 were men. This leaves us with no obvious factor linking the samples together other than variation during sample preparation.

Further more detailed evaluation of these results using bioinformatics is required but it is beyond the scope of this report due to time limitations.

5.2 Biomechanics

In order to obtain large enough force levels required by the force cell of 250N, the samples chosen needed to be of a certain size. As the medial samples were generally more degenerated, the plug diameter did not as often contain 8 mm in diameter of tissue, thus we focused on lateral menisci. However, the drawback was of course that the lateral menisci were generally less osteoarthritic. This explains why no certain difference in the biomechanical properties between lateral meniscus tissue from healthy and osteoarthritic knee was found. According to theory, the compressive modulus, and therefore also the aggregate modulus, should decrease with increasing degeneration of the menisci [36] [45]. This is however not something that could be observed from our experiment.

As mentioned, a certain magnitude of the force is required for different load cells. A load cell is calibrated down to about 0.5% of its capacity, with an accuracy of 0.5% of the read-out values. Thus, for future tests where smaller punches will be used, a more sensitive force cell should be used.

A factor that could have affected the biomechanical results is the fact that, in some cases, a few samples were placed just on the border of the indenter. This has been noted for sample 007L, however, the results for this sample are largely similar to the other samples.

Prior to commencing the loading protocol, PBS was used in order to keep the samples hydrated for the total duration of the testing. It seems unlikely that the presence of PBS surrounding the sample should affect the forces withstood by the menisci, however, it can be discussed whether or not these conditions correspond to the physiological environment of the knee. Since our biomechanical results were primarily used for internal comparisons between the mensici with varying degeneration, the importance lied in maintaining consistency and reproducibility rather than replicating the in vivo conditions.

The pre-load was set to 0.3 N, 6kPa, for all samples in order to ensure contact between the sample and the plate as well as providing positional control. This pre-load was chosen after literature research [46][47] and

protocol testing. For some cases, the pre-load might have been too high relative to the first peak value, resulting in an unreasonably high relaxation ratio in many cases. With this in mind, the relaxation ratio for peak 2-4 seen in table 4.1 and 4.2 are more representative.

The relaxation time was predetermined to when the tissue relaxed less than 150 Pa/min. Unfortunately, this criterion was not satisfied in many of the cases and the relaxation time was instead calculated by implementing a material model.

5.2.1 Material modelling

Visually, the Generalized Maxwell model with two Maxwell elements was a good curve fit for the biomechanical data. Through the material modelling, the parameters E_0,E_1, E_2, τ_1 and τ_2 were obtained for all samples.

As expressed in equation 2.4, the springs E_0, E_1 and E_2 are responsible for the initial stress response when the system is exposed to a sudden strain. Both E_1 and E_2 can be described as strain level dependent as they, for the majority of the samples, increase with each peak. This is expected since a higher strain should lead to a higher stress in the system.

For all living materials, a single characteristic time is often not accurate enough which is why this model incorporates two time constants, τ_1 and τ_2. They represent molecular strands with varying lengths found in tissues and therefore contribute to the relaxation to varying degrees. As our results show, for each sample, τ_1 has a considerably lower value than τ_2. Another pattern that can be seen for the majority of the samples is that both τ_1 and τ_2 continuously increase with an increase in strain. When analysing the impact of τ_1 and τ_2 on the relaxation curve, it can be noted that τ_1 has an effect on the immediate response, a larger τ_1 causes a less steep initial decline. τ_2 affects the curve's behaviour over time and is considerably more responsible for the tissue's total relaxation time. A larger τ_2 should therefore lead to an overall longer relaxation time in the tissue. This explains and supports the general observation that with increasing strain, both τ_2 and therefore even the relaxation time, increases.

As time elapses and when the dashpots have undergone full relaxation, the remaining stress is constituted by the single spring, E_0. This ultimately means that a lower E_0 implies a more complete relaxation of the tissue. The spread of the values for E_0 makes it difficult to interpret the results and to draw any conclusions. The anticipation was that the residual stress, i.e. E_0, would correlate with the strain level.

With a a larger number of parallel Maxwell components, the data fitting can be made more accurate, however, this quickly increases the mathematical complexity. The physiological interpretation also becomes less comprehensible the more springs and dashpots that are added to the system. Finding the right balance between an accurate model fit and a suitable complexity is therefore of interest when choosing model. For this experiment, two Maxwell components was considered a favourable choice.

In the same manner as the results from the biomechanical testing showed, we find it difficult to see any differences between the mechanical properties of menisci from healthy and osteoarthritic knees. However, the parameters obtained from the Generalized Maxwell model are realistic and correspond well to the overall expected outcome.

5.3 Biomechanics related to proteomics

The proteomic findings of up and down regulated proteins can be linked to overall weakened compressive forces in the menisci from osteoarthritic knees. However, this hypothesis can not be strengthened in our report since our mechanical results concerning Young's modulus and aggregate modulus were unconvincing. Our biomechanical experiment was, as previously mentioned, solely based on lateral menisci and, as the protein regulation demonstrated, the most considerable differences were seen in medial menisci. Due to this, we find it hard to draw conclusions regarding the protein content in relation to the biomechanical properties and suggest that further research should instead focus on the medial menisci, provided adequate amounts of tissue can be obtained for biomechanical testing.

The heatmap showed no clustering between the groups with respect to age, sex or BMI. This was somewhat unexpected but could most likely be explained by the small sample size. With a larger number of samples, there may be patterns both with regards to the protein content and the biomechanical properties. In order to properly investigate how age, sex and BMI potentially affect the meniscal properties with degeneration, a considerably larger sample size would have been required.

5.4 Ethical aspects

The purpose of this project was to examine the degeneration of menisci during the progression of OA and evaluate the mechanical effects. Since OA is such a prevalent disease, the possibility of gaining further understanding of the disease progression would be of great benefit to a large proportion of the population, supporting the intention of this project.

When dealing with human tissue, it is essential that respect is shown and that the samples are handled with care. An aspect that needs to be taken into account is the assessment of the risks and the benefit. The menisci used in this study were from both osteoarthritic patients undergoing total knee replacement surgery and deceased donors. Prior to surgery, all the patients gave consent to allowing their menisci to be used for research purposes, rather than discarding them. As the menisci were removed anyway (during the routine surgical procedure), there was no additional risk of physical harm to the patients. The healthy menisci were provided through registered organ donors or deceased individuals whose closest relatives gave consent to preserve the organs for research purposes.

Total anonymity has been secured during this study. No personal information has been spread and the metadata from each individual has been de-identified.

The biobank providing the meniscal samples and the examinations of these samples has passed ethical review at the regional ethics committee in Lund (Dnr 2015/39 and 2016/865) and national ethical review authority (Dnr 2019-00323).

Chapter 6

Conclusions

In this project we have successfully measured and evaluated the protein content for 50 menisci, 20 from healthy knees and 30 from osteoarthritic knees. Further, we developed a protocol and tested the biomechanical properties through unconfined compression for 12 lateral menisci, 6 from healthy knees and 6 from osteoarthritic knees.

We found that the lateral menisci suffer overall minimal degeneration in knees with medial compartment end-stage OA, both with respect to the proteome as well as the biomechanical properties. Due to the medial meniscus often being more destructed in medial compartment OA, finding subjects with sufficient meniscal tissue preserved to allow for mechanical testing is challenging. Further experiments may e.g. consider using a load cell adapted for lower forces, allowing smaller punches to be taken in the meniscus remnants, or identifying a group of subjects with medial compartment OA at an earlier disease stage.

Bibliography

[1] M. Englund and A. Turkiewicz. Artros allt vanligare folksjukdom. `https://lakartidningen.se/klinik-och-vetenskap-1/artiklar-1/klinisk-oversikt/2014/05/artros-allt-vanligare-folksjukdom/`. [Online; accessed 2021-03-20].

[2] N. Ali, A. Turkiewicz, V. Hughes, E. Folkesson, J. Tjörnstand, P. Neuman, P. Önnerfjord, and M. Englund. Proteomics profiling of human synovial fluid suggests global increased protein interplay in early-osteoarthritis (oa) and lost in late-stage oa. *bioRxiv*, 2020.

[3] P. H. Finan, L. F. Buenaver, S. C. Bounds, S Hussain, R. J. Park, U. J. Haque, C. M. Campbell, J. A. Haythornthwaite, R. R. Edwards, and M. T. Smith. Discordance between pain and radiographic severity in knee osteoarthritis. *Arthritis and rheumatism*, 65(2), Feb 2013.

[4] Y. Zhang and J. M. Jordan. Epidemiology of osteoarthritis. *Clinics in geriatric medicine*, 26(3):355–369, Aug 2010.

[5] C. A. Murphy, A. K. Garg, J. Silva-Correia, R. L. Reis, J. M. Oliveira, and M. N. Collins. The meniscus in normal and osteoarthritic tissues: Facing the structure property challenges and current treatment trends. *Annual Review of Biomedical Engineering*, 21(1):495–521, 2019. PMID: 30969794.

[6] M. Englund, I.K. Haugen, A. Guermazi, F.W. Roemer, J. Niu, T. Neogi, P. Aliabadi, and D.T. Felson. Evidence that meniscus damage may be a component of osteoarthritis: the framingham study. *Osteoarthritis and Cartilage*, 24(2):270–273, 2016.

[7] D. J Hunter and F. Eckstein. Exercise and osteoarthritis. *Journal of Anatomy*, 214(2):197–207, Feb 2009.

[8] M. Englund, A. Guermazi, and S. L. Lohmander. The role of the meniscus in knee osteoarthritis: a cause or consequence? *Radiologic Clinics of North America*, 47(4):703–712, Jul 2009.

[9] S. P Yu and D. J Hunter. Managing osteoarthritis. *Australian Prescriber*, 38(4):115–119, Aug 2015.

[10] I. J. Wallace, S. Worthington, D. T. Felson, R. D. Jurmain, K. T. Wren, H. Maijanen, R. J. Woods, and D. E. Lieberman. Knee osteoarthritis has doubled in prevalence since the mid-20th century. *Proceedings of the National Academy of Sciences of the United States of America*, 114(35):9332–9336, Aug 2017.

[11] A. J. Fox, F. Wanivenhaus, A. J. Burge, R. F. Warren, and S. A. Rodeo. The human meniscus: A review of anatomy, function, injury, and advances in treatment. *Clinical Anatomy*, 28(2):269–287, 2015.

[12] Southern Suburbs Physio Centre. Arthroscopic meniscus surgery is it finished? `https://www.sspc.com.au/inteligent-transitions-in-ux-design-2/`. [Online; accessed 2021-05-06].

[13] F. Mahmood, J. Clarke, and P. Riches. Proteoglycans exert a significant effect on human meniscal stiffness through ionic effects. *Clinical Biomechanics*, 77:105028, 2020.

[14] A. J. Fox, A. Bedi, and S. A. Rodeo. The basic science of human knee menisci: structure, composition, and function. *Sports health*, 4(4):340–351, 2012.

[15] R. Howell, N. S. Kumar, N. Patel, and J. Tom. Degenerative meniscus: Pathogenesis, diagnosis, and treatment options. *World journal of orthopedics*, 5(5):597–602, 2014.

[16] A. J. S. Fox, A. Bedi, and S. A. Rodeo. The basic science of human knee menisci. *Sports Health*, 4(4):340–351, Jul 2012.

[17] C. T. Thorpe, H. L. Birch, P. D. Clegg, and H. R.C. Screen. Chapter 1 - tendon physiology and mechanical behavior: Structure–function relationships. In Manuela E. Gomes, Rui L. Reis, and Márcia T. Rodrigues, editors, *Tendon Regeneration*, pages 3–39. Academic Press, Boston, 2015.

[18] T. E. Gould, M. Jesunathadas, S. Nazarenko, and S. G. Piland. Chapter 6 - mouth protection in sports. In Aleksandar Subic, editor, *Materials in Sports Equipment (Second Edition)*, Woodhead Publishing Series in Composites Science and Engineering, pages 199–231. Woodhead Publishing, second edition edition, 2019.

[19] ThermoFischer Scientific. Protein sample preparation for mass spectrometry. `https://www.thermofisher.com/se/en/home/life-science/protein-biology/protein-biology-learning-center/protein-biology-resource-library/pierce-protein-methods/sample-preparation-mass-spectrometry.html`. [Online; accessed 2021-03-30].

[20] ThermoFischer Scientific. Liquid chromatography mass spectrometry (lc-ms) information. `https://www.thermofisher.com/se/en/home/industrial/mass-spectrometry/mass-spectrometry-learning-center/liquid-chromatography-mass-spectrometry-lc-ms-information.html`. [Online; accessed 2021-03-30].

[21] Shimadzu. Fundamentals of lc, ms and lcms. `https://www.shimadzu.com/an/service-support/technical-support/analysis-basics/fundamental/ms_and_lcms.html`. [Online; accessed 2021-04-26].

[22] C. Dass. *Fundamentals of Contemporary Mass Spectrometry*. John Wiley Sons, Inc., 2006.

[23] X. Han, A. Aslanian, and J. R. Yates 3rd. Mass spectrometry for proteomics. *Current opinion in chemical biology*, 12(5):483–490, Oct 2008.

[24] A. Lahesmaa-Korpinen. *Computational approaches in high-throughput proteomics data analysis*. PhD thesis, Jun 2012.

[25] G. Büyükköroğlu, D. D. Dora, F. Özdemir, and C. Hızel. Chapter 15 - techniques for protein analysis. In Debmalya Barh and Vasco Azevedo, editors, *Omics Technologies and Bio-Engineering*, pages 317–351. Academic Press, 2018.

[26] L. Krasny and P. H. Huang. Data-independent acquisition mass spectrometry (dia-ms) for proteomic applications in oncology. *Molecular omics*, 17(1):29–42, Feb 2021.

[27] H. Lim and S. Hoag. Plasticizer effects on physical–mechanical properties of solvent cast soluplus® films. *AAPS PharmSciTech*, 14, May 2013.

[28] The Editors of Encyclopaedia Britannica. Young's modulus. `https://www.britannica.com/science/Youngs-modulus`. [Online; accessed 2021-04-22].

[29] J. Mansour. *Biomechanics of cartilage*, pages 69–83. Jul 2013.

[30] R. Korhonen and S. Saarakkala. *Biomechanics and Modeling of Skeletal Soft Tissues*. Nov 2011.

[31] Qinwu Xu and Björn Engquist. A mathematical model for fitting and predicting relaxation modulus and simulating viscoelastic responses. *Proceedings of the Royal Society A: Mathematical, Physical and Engineering Sciences*, 474(2213):20170540, May 2018.

[32] D. J. Hunter, E. Losina, A. Guermazi, D. Burstein, M. N. Lassere, and V. Kraus. A pathway and approach to biomarker validation and qualification for osteoarthritis clinical trials. *Current Drug Targets*, 11(5):536–545, May 2010.

[33] E. Folkesson, A. Turkiewicz, N. Ali, M. Rydén, V. Hughes, J. Tjörnstrand, P. Önnerfjord, and M. Englund. Proteomic comparison of osteoarthritic and reference human menisci using data-independent acquisition mass spectrometry. *Osteoarthritis and Cartilage*, 28(8):1092–1101, 2020.

[34] C. Pauli, S.P. Grogan, S. Patil, S. Otsuki, A. Hasegawa, J. Koziol, M.K. Lotz, and D.D. D'Lima. Macroscopic and histopathologic analysis of human knee menisci in aging and osteoarthritis. *Osteoarthritis and cartilage / OARS, Osteoarthritis Research Society*, 19(9):1132–1141, Sep 2011.

[35] Y. Katsuragawa, K. Saitoh, N. Tanaka, M. Wake, Y. Ikeda, H. Furukawa, S. Tohma, M. Sawabe, M. Ishiyama, S. Yagishita, and et al. Changes of human menisci in osteoarthritic knee joints. *Osteoarthritis and Cartilage*, 18(9):1133–1143, Sep 2010.

[36] K. Fischenich, J. Lewis, K. Kindsfater, T. Bailey, and T. Donahue. Effects of degeneration on the compressive and tensile properties of human meniscus. *Journal of Biomechanics*, 48, Feb 2015.

[37] Y. S. Lai, W. C. Chen, C. H. Huang, C. K. Cheng, K. K. Chan, and T. K. Chang. The effect of graft strength on knee laxity and graft in-situ forces after posterior cruciate ligament reconstruction. *PLOS ONE*, 10:e0127293, May 2015.

[38] X. Chang, J. Han, Y. Zhao, X. Yan, S. Sun, and Y. Cui. Increased expression of carbonic anhydrase i in the synovium of patients with ankylosing spondylitis. *BMC Musculoskeletal Disorders*, 11:279, Dec 2010.

[39] E. A. Makris, P. Hadidi, and K. A. Athanasiou. The knee meniscus: structure-function, pathophysiology, current repair techniques, and prospects for regeneration. *Biomaterials*, 32(30):7411–7431, Oct 2011.

[40] P. Bornstein, A. Agah, and T. R. Kyriakides. The role of thrombospondins 1 and 2 in the regulation of cell–matrix interactions, collagen fibril formation, and the response to injury. *The International Journal of Biochemistry Cell Biology*, 36(6):1115–1125, 2004. Modulatory Adhesion Molecules in Tissue Homeostasis.

[41] H. S. Kwon, T. V. Johnson, and S. I. Tomarev. Myocilin stimulates osteogenic differentiation of mesenchymal stem cells through mitogen-activated protein kinase signaling. *The Journal of Biological Chemistry*, 288(23):16882–16894, Jun 2013.

[42] T. Mine, K. Ihara, H. Kawamura, R. Date, and K. Umehara. Collagen expression in various degenerative meniscal changes: An immunohistological study. *Journal of Orthopaedic Surgery*, 21(2):216–220, 2013.

[43] G. Smyrnova. The relationship between hemoglobin level and disease activity in patients with rheumatoid arthritis. *Revista Brasileira De Reumatologia*, 54(6):437–440, Dec 2014.

[44] B. C. Bernardo, D. Belluoccio, L. Rowley, C. B. Little, U. Hansen, and J. F. Bateman. Cartilage intermediate layer protein 2 (cilp-2) is expressed in articular and meniscal cartilage and down-regulated

in experimental osteoarthritis. *Journal of Biological Chemistry*, 286(43):37758–37767, Oct 2011.

[45] D. Warnecke, J. Balko, J. Haas, R. Bieger, F. Leucht, N. Wolf, N.B. Schild, S.E.C. Stein, A.M. Seitz, A. Ignatius, H. Reichel, B. Mizaikoff, and L. Dürselen. Degeneration alters the biomechanical properties and structural composition of lateral human menisci. *Osteoarthritis and Cartilage*, 28(11):1482–1491, 2020.

[46] J. Ala-Myllymäki, E. K. Danso, J. T. J. Honkanen, R. K. Korhonen, J. Töyräs, and I. O. Afara. Optical spectroscopic characterization of human meniscus biomechanical properties. *Journal of Biomedical Optics*, 22(12):1 – 10, 2017.

[47] R.K Korhonen, M.S Laasanen, J Töyräs, J Rieppo, J Hirvonen, H.J Helminen, and J.S Jurvelin. Comparison of the equilibrium response of articular cartilage in unconfined compression, confined compression and indentation. *Journal of Biomechanics*, 35(7):903–909, 2002.

Appendix

Mass Spectrometry settings

DIA settings: method duration 125 min, full scan resolution 120 000, scan range 350-1650 m/z. AGC target 3.0e6, maximum injection time 100 ms, Orbitrap resolution 45 000, AGC 3.0e5 with a variable isolation window 33/ 26/ 22/ 20x2/ 18/ 20/ 19x4/ 20/ 21x2/ 23x2/ 24/ 26/ 31/ 32/ 37/ 40/ 53/ 66/ 99/ 574 m/z, and normalized collision energy 27 eV.

DDA settings: method duration 125 min, mass range 350-1650 m/z., full MS scan resolution 120 000, AGC 3e6, maximum injection time 20 ms, Orbitrap resolution 15 000, AGC target 1.0e5, maximum injection 20ms, normalized collision energy 27 eV.

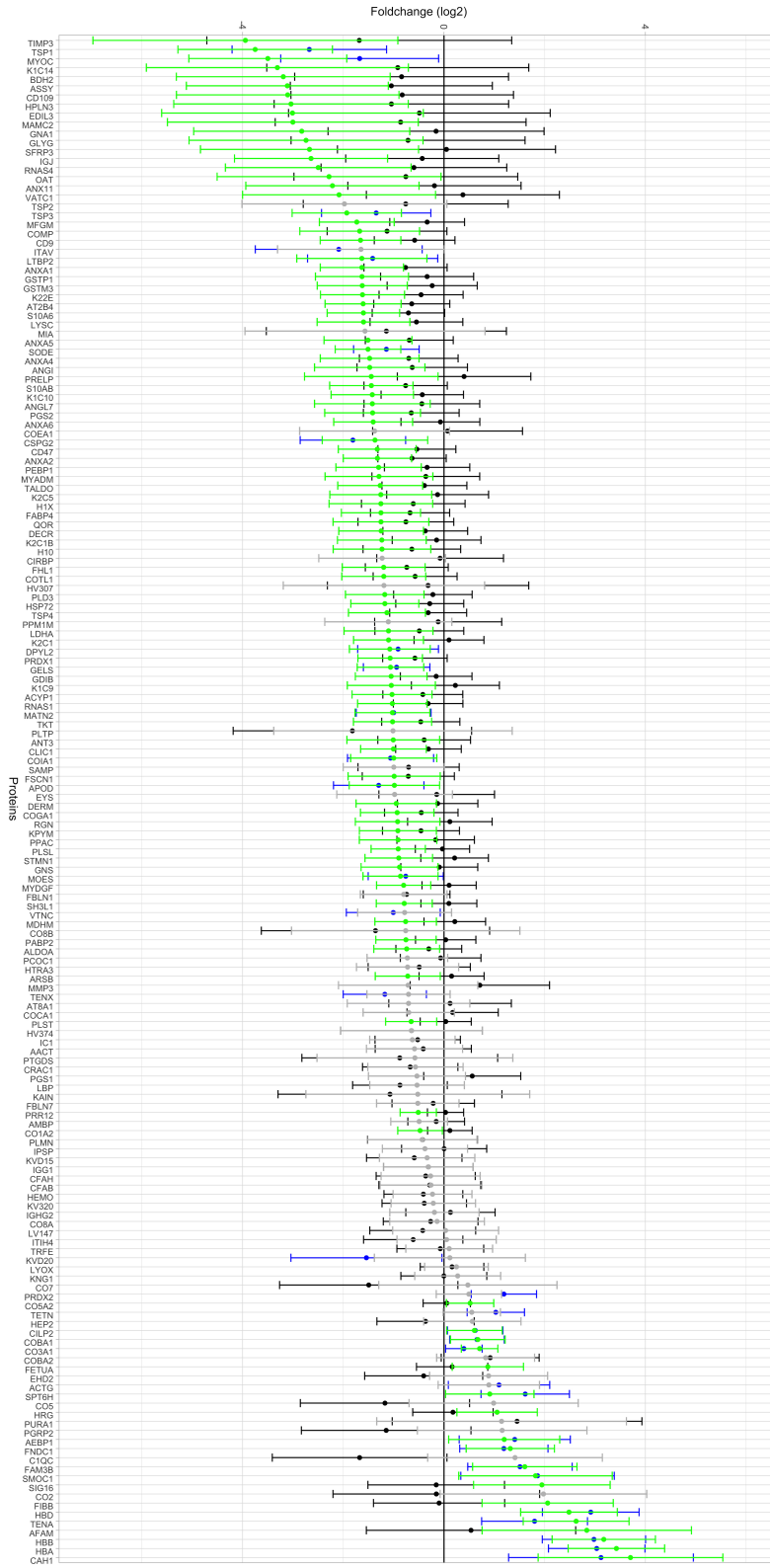

Figure 7.1: Protein regulation of menisci from arthritic knees in relation to healthy knees.